

# 1

## An Introduction to Bio-nanohybrid Materials

Eduardo Ruiz-Hitzky, Margarita Darder, Pilar Aranda

### 1.1

#### Introduction: The Assembly of Biological Species to Inorganic Solids

The assembly of molecular or polymeric species of biological origin and inorganic substrates through interactions on the nanometric scale constitutes the basis for the preparation of bio-nanohybrid materials (Figure 1.1). The development of these materials represents an emerging and interdisciplinary topic at the border of Life Sciences, Material Sciences and Nanotechnology. They are of great interest due to their versatile applications in important areas as diverse as regenerative medicine and new materials with improved functional and structural properties [1–5]. It must be remarked that the development of bio-nanocomposites also represents an ecological alternative to conventional polymer nanocomposites, as the properties of the biodegradable polymers used ensure that the materials produced are environmentally friendly and renewable. Typical examples of this type of bio-nanocomposites result from the combination of polysaccharides such as starch, cellulose or polylactic acid (PLA) with microparticulated solids, which are usually called *green nanocomposites* or *bioplastics* [6,7].

Recently, special attention has been paid to strategies for synthetic approaches to bio-nanohybrids. One of these approaches is related to the preparation of bioinspired or biomimetic materials following the examples found in Nature, as for instance, bone [8], ivory [9] and nacre [10–13]. These materials show excellent structural properties due to the special arrangement at the nanometric level of their assembled components, that is biopolymers and inorganic counterparts. For instance, nacre represents a good example of a natural bio-nanocomposite, also known as *native biomaterial*, formed by the stacking of highly oriented calcium carbonate (aragonite) platelets cemented by a fibrous protein (lustrin A). The resulting supra-architectures show exceptional mechanical properties compared to monolithic calcium carbonate [11,12].

Nowadays, bio-nanocomposites mimicking these natural materials have been prepared with the aim being to develop new biohybrids with improved mechanical properties together with biocompatibility and, in some cases, other interesting

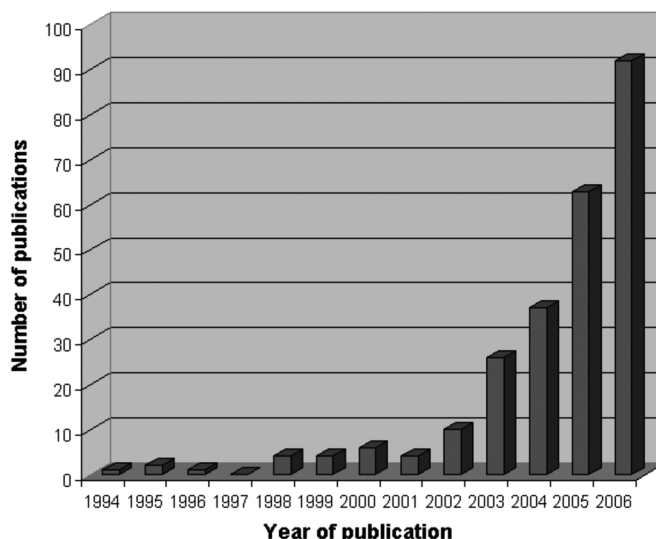


**Fig. 1.1** Number of publications per year related to bio-nanohybrid materials. Data collected from the ISI Web of Knowledge [v3.0]-Web of Science. Keywords for search: (biopolymer\* AND nanocomposite\*) OR (natural polymer\* AND nanocomposite\*) OR (bio-nanohybrid\*) OR (biohybrid\* AND nano\*).

features such as functional behavior [14–18]. In this context, the development of biohybrid systems based on biomimetic building [18,19], that is following biomineralization processes similar to those that take place in the cell wall of diatoms, where nanostructured silica nanospheres are assembled by the participation of cationic polypeptides called silaffins (SILica AFFINity) [20,21] appears to be of great significance. In relation to these natural systems, the mechanisms of interaction between colloidal silica and peptides have been particularly studied with the aim being to understand the biomineralization processes and consequently to develop, in a controlled manner, new improved synthetic bio-nanocomposites [22–24].

Inorganic solids assembled with biological species are of diverse nature with different chemical compositions, structures and textures, which determine the properties of the resulting bio-nanohybrids. In this way, single elements such as transition metals and carbon particles, metal oxides and hydroxides, silica, silicates, carbonates and phosphates, are typical inorganic components of bio-nanohybrids (Table 1.1). The affinity between the inorganic and the bio-organic counterparts, which determines the stability of the resulting bio-composites, depends on the interaction mechanisms governing the assembly processes.

As indicated above, the development of bio-nanohybrids by mimicking biomineralization represents an extraordinarily useful approach. This is, for instance, the case for those bio-nanocomposites based on bone biomimetic approaches, which show excellent structural properties and biocompatibility. They are prepared by

**Tab. 1.1** Selected Examples of Bio-Nanohybrid Materials Involving Different Types of Inorganic Solids.

Inorganic moiety	Biological species	Bio-nanohybrid features	Authors/References
silica nanoparticles	poly-L-lysine (PLL)	biomimetic nanocomposites with controlled morphology	Patwardhan <i>et al.</i> [39]
siloxane networks	living bacteria	encapsulation by sol-gel	Fennouh <i>et al.</i> [62]
calcium carbonate hydroxyapatite (HAP)	chitosan and poly(aspartate) collagen	biomimetic preparation towards artificial nacre biomimetic porous scaffolds for bone regeneration	Sugawara and Kato [88] Yokoyama <i>et al.</i> [94]
layered clay minerals (montmorillonite)	chitosan	functional bio-nanocomposite for ion-sensing applications	Darder <i>et al.</i> [129]
fibrous clay minerals (sepiolite)	caramel	bio-nanocomposite as precursor of multifunctional carbon–clay nanostructured materials	Gómez-Avilés <i>et al.</i> [153]
organoclays	PLA	green nanocomposites as biodegradable bioplastics	Paul <i>et al.</i> [144]
layered double hydroxides (LDHs)	deoxyribonucleic acid (DNA)	bio-nanocomposite as non-viral vector for gene transfection	Choy <i>et al.</i> [159]
gold nanoparticles	chitosan	bio-nanohybrid processable as self-supporting films for biosensor applications	dos Santos <i>et al.</i> [164]
magnetite nanoparticles	phosphatidylcholine	<i>magnetocerasomes</i> for targeted drug delivery	Burgos-Asperilla <i>et al.</i> [73]
carbon nanotubes (CNTs)	galactose	modified CNTs able to capture pathogens by protein binding	Gu <i>et al.</i> [194]
layered perovskites ( $\text{CsCa}_2\text{Nb}_3\text{O}_{10}$ )	gelatin	bio-nanocomposite thin films with dielectric properties	Ruiz <i>et al.</i> [220]

assembling hydroxyapatite (HAP), which is the main mineral constituent of bones and teeth, with biopolymers, for example collagen [25–27]. The coating of the micro- or nano-particulated solids with biopolymers often occurs through hydrogen-bonding or metal-complexing mechanisms. In this way, the assembly of magnetic iron oxide nanoparticles (e.g., magnetite) with biopolymers (e.g., dextran) allows the preparation of magnetic bio-nanocomposites applied in NMR imaging, hyperthermia treatments or bio-carriers as drug delivery systems (DDS) [28,29].

The assembly of biopolymers with inorganic layered solids can lead to bio-nanocomposites in which the biopolymer becomes intercalated between the layers of the inorganic hosts [3]. The intercalation is a complex process that may simultaneously involve several mechanisms. Thus, in addition to hydrogen bonding, it has been invoked that certain biopolymers interact with the inorganic layers through

ionic bonds. This is the case for polysaccharides, proteins and nucleic acids that can act as polyelectrolytes intercalating, via ion-exchange reaction, solids provided with positively or negatively charged layers, such as layered double hydroxides (LDHs) or smectite clay minerals (see below).

Microfibrous crystalline silicates such as sepiolite, similarly to amorphous silica, contain silanol groups (Si–OH) covering the external mineral surface. These groups can be effectively involved in hydrogen bonding by their association to OH, NH and other polar groups belonging to the biopolymers used. Silica generated by the sol–gel method from tetraethyl orthosilicate (TEOS) in the presence of chitosan, gives biopolymer-silica nanocomposites whose morphology can be determined by the experimental conditions adopted for the preparation [30]. Chitosan and collagen can also be assembled with sepiolite to give the corresponding biopolymer–sepiolite nanocomposites, which exhibit good mechanical properties resulting from the combination of the fibrous inorganic substrate with the biopolymer [31–34]. The interaction mechanisms governing the formation of sepiolite-based bio-nanocomposites are mainly ascribed to hydrogen bonding, but it must be taken into account that sepiolite exhibits cationic exchange capacity (CEC  $\sim$ 15 meq/100 g). Thus this silicate could also interact with positively charged polymers, such as chitosan, through electrostatic bonds.

Although to only a minor extent, other mechanisms can be invoked, as for instance covalent bonding (grafting) between hydroxy groups on the surface of the inorganic substrates and functional groups of the biopolymers [35].

The aim of this chapter is to provide a general overview of the preparation and main characteristics of bio-nanohybrids, with emphasis on the different types of inorganic solids that can be involved in the formation of this class of materials. Special attention will be devoted to the diverse mechanisms that govern the interaction between the components of biohybrids, illustrating them with selected examples. Relevant features and potential or actual applications of recently developed bio-nanocomposites will be discussed on the basis of their structure–property relationships.

## 1.2

### Bio-nanohybrids Based on Silica Particles and Siloxane Networks

Biominerals are produced by living organisms following a set of processes known as biominerization, which results in a wide variety of biological materials including shells, bones, teeth, ivory and magnetic nanoparticles in magnetotactic bacteria. Biomolecules secreted by living organisms control the nucleation and growth of inorganic minerals (carbonates, phosphates, silica and iron oxide) leading to such a diversity of biological-inorganic hybrid materials, which usually exhibit a hierarchical arrangement of their components from the nanoscale to the macroscopic scale. The skeletons of diatoms and radiolarians are astonishing examples of biosilicification giving rise to amorphous hydrated  $\text{SiO}_2$  (biosilica), also formed in sponges and many higher plants [24]. As mentioned in Section 1, polycationic peptides, called silaffins, are involved in this process, controlling the assembly of silica nanoparticles to form

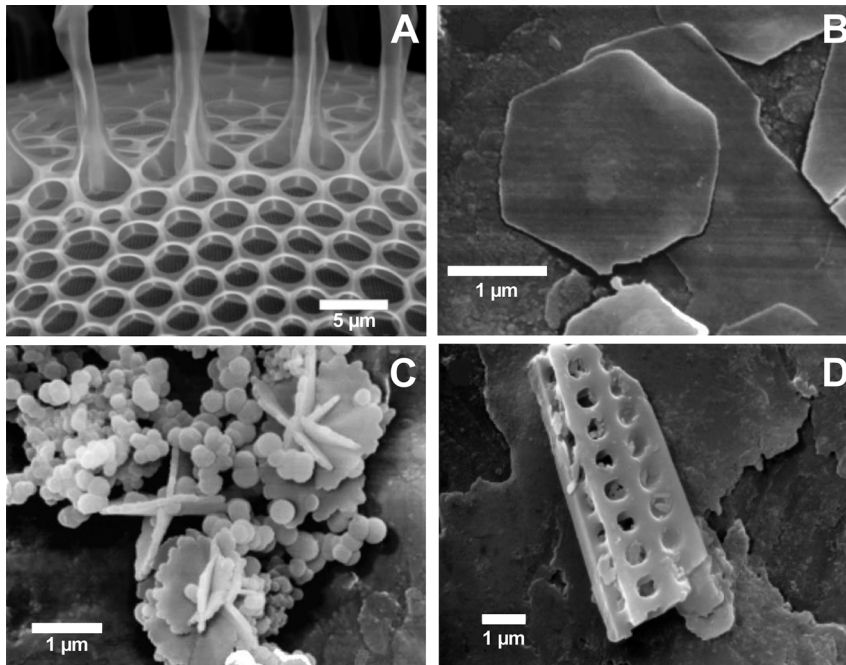


**Fig. 1.2** Scanning electron micrographs of (A) the silica wall of the diatom *Stephanopyxis turris* (reproduced from [21] by permission of Wiley-VCH) and (B–D) singular morphologies of silica synthesized using poly-L-lysine and pre-hydrolyzed tetramethyl orthosilicate (TMOS) under

different experimental conditions: (B) unperturbed solution, (C) flowed through a 1/8" I.D. tube and (D) stirred for 25 min. Reproduced from [39] by permission of The Royal Society of Chemistry.

these siliceous structures [20,21,36]. Similarly, silica needles in the skeleton of marine sponges involve a central filament containing silicatein, an enzyme that catalyses the synthesis of biosilica [37]. Materials scientists try to understand and reproduce these biosilicification processes taking place in nature, with the aim being to develop bioinspired or biomimetic hybrid nanostructured materials with controlled morphologies and structural properties similar to those of biosilica [24,38–42], as shown in Figure 1.2. As recently reviewed by Coradin *et al.* [43], proteins (collagen, gelatin, and silk) and polysaccharides (alginate, carrageenans, chitosan, as well as cellulose and its derivatives) are the main biomacromolecules involved in the synthesis of biopolymer/silica nanocomposites, while silicic acid, sodium silicate and different silicon alkoxides are employed as precursors of the silica or the polysiloxane networks assembled with the biopolymer chains. Following biomimetic processes, lysozyme and bovine serum albumin (BSA) promote the precipitation of silica particles from sodium silicate solutions, leading to entrapment of the protein [44]. Similarly, polysaccharides such as cationic and hydrophobic derivatives of cellulose also promote silica precipitation, acting as efficient templates to

develop organic–inorganic hybrid nanocomposites in combination with tetrakis(2-hydroxyethyl)orthosilicate (THEOS) [45]. Chitosan is another natural polysaccharide involved in this type of silica-based hybrid material prepared by the sol–gel method. For instance, it has been assembled with siloxane networks derived from amino-propylsiloxane (APS) [46] or TEOS [30]. A similar chitosan–polysiloxane biohybrid material has been recently prepared from chitosan and 3-isocyanatopropyltriethoxysilane, where chitosan is bound to the polysiloxane network by covalent bridges. This new functional material offers photoluminescent features and bioactive behavior, since it promotes apatite formation in simulated body fluid [47]. Chitosan–silica hybrids present as microparticulate materials showing different shapes have been prepared by the sol–gel method using TEOS or polyethoxysiloxane oligomers in the presence of the biopolymer. These materials can be used as a stationary phase in HPLC [48].

In these examples as well as in analogous materials, the interaction of the biological and the inorganic components has synergistic effects leading to hybrid materials with improved mechanical resistance, higher thermal and chemical stability and biocompatibility, and, in some cases, with functional properties. Biopolymer/silica nanocomposites are suitable for the design of membranes and coatings, drug delivery systems and also for the encapsulation of bioactive molecules such as enzymes, antibodies, yeast and plant cells or even bacteria, resulting in functional biomaterials for different biotechnological applications, including biosensors and bioreactors [43,49].

Silica-based bio-nanocomposites for drug delivery purposes have been processed as nanospheres by means of spray-drying or  $\text{CO}_2$  supercritical drying techniques. Hybrid nanoparticles based on algal polysaccharides such as alginate and carrageenan are potential carriers for the targeted delivery of drugs due to their ability to go into the intracellular space of cells and to their lack of cytotoxicity [50,51]. In other cases, silica nanoparticles serve as a support of biocide molecules and their dispersion in hydroxypropylcellulose allows the preparation of coatings and films with fungicide and pesticide activity [52]. Following a similar approach, Zhang and Dong [53] have developed functional materials based on the dispersion of  $\text{Ru}(\text{bpy})_3^{2+}$ -doped silica nanoparticles in the biopolymer chitosan. The resulting hybrid material can be easily spread onto the surface of electrodes as a stable electroactive coating, allowing the development of chemiluminescence sensors.

Similarly to the above-mentioned entrapment of proteins by biomimetic routes, the sol–gel procedure is a useful method for the encapsulation of enzymes and other biological material due to the mild conditions required for the preparation of the silica networks [54,55]. The confinement of the enzyme in the pores of the silica matrix preserves its catalytic activity, since it prevents irreversible structural deformations in the biomolecule. The silica matrix may exert a protective effect against enzyme denaturation even under harsh conditions, as recently reported by Frenkel-Mullerad and Avnir [56] for physically trapped phosphatase enzymes within silica matrices (Figure 1.3). A wide number of organoalkoxy- and alkoxy-silanes have been employed for this purpose, as extensively reviewed by Gill and Ballesteros [57], and the resulting materials have been applied in the construction of optical and electrochemical biosensor devices. Optimization of the sol–gel process is required to prevent denaturation of encapsulated enzymes. Alcohol released during the

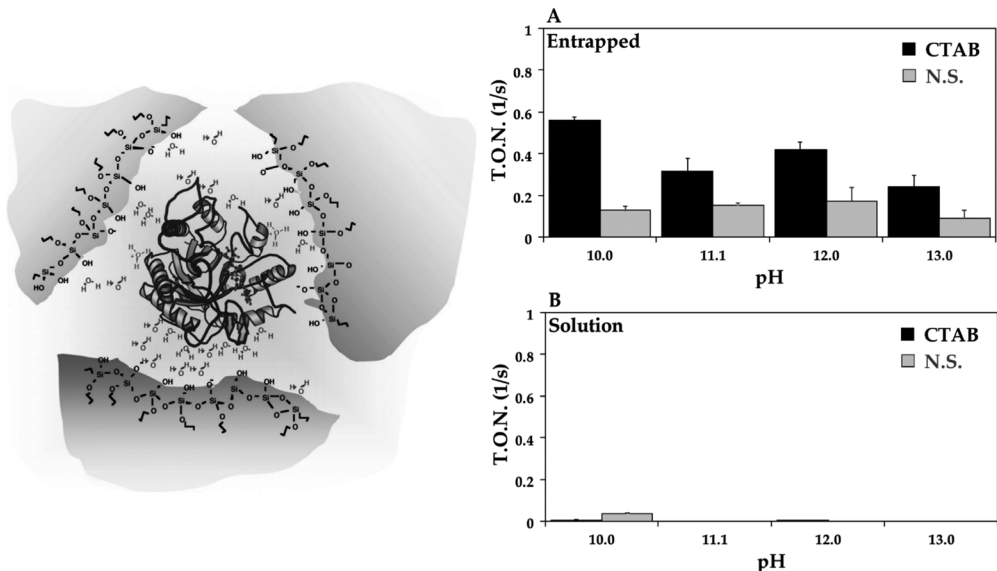


**Fig. 1.3** Schematic representation of the entrapped enzyme in a silica matrix (left side). Enzymatic activity, under extreme alkaline conditions, of acid phosphatase (A) immobilized in silica sol-gel matrices with or without CTAB, or (B) in solution. Reprinted with permission from [56]. Copyright 2005, American Chemical Society.

hydrolysis process can be harmful for the entrapped biologicals and, thus, several methods propose its removal by evaporation under vacuum [58] or the use of polyol-based silanes that generate biocompatible alcohols [59]. Catalytic activity is also preserved when silica-polysaccharide bio-nanocomposites are used as immobilization hosts. This is the case for three-dimensional hybrid matrices resulting from the combination of THEOS with xanthan, locust bean gum or a cationic derivative of hydroxyethylcellulose, which have been reported as excellent networks for the long-term immobilization of  $1 \rightarrow 3$ - $\beta$ -D-glucanase and  $\alpha$ -D-galactosidase [60].

In addition to enzymes and antibodies, silica-based hybrid nanocomposites with a suitable porosity can successfully entrap more complex systems including yeasts, algae, lichens, plant cells and bacteria [49]. The huge volume of biological tissues, in comparison to enzymes, may hinder the polymerization processes resulting in fractures in the silica matrices. To overcome this drawback, lichen particles were embedded in a flexible network, derived from 3-(trimethoxysilyl)propyl methacrylate (MAPTS) and tetramethoxysilane (TMOS), that offers improved mechanical features (Figure 1.4A). This lichen-modified material was used to develop electrochemical sensors for the determination of heavy metal ions by anodic stripping voltammetry [61]. Similarly, algal tissue can be immobilized in sol-gel derived matrices based on TMOS and methyltrimethoxysilane (MTMOS) (Figure 1.4B).

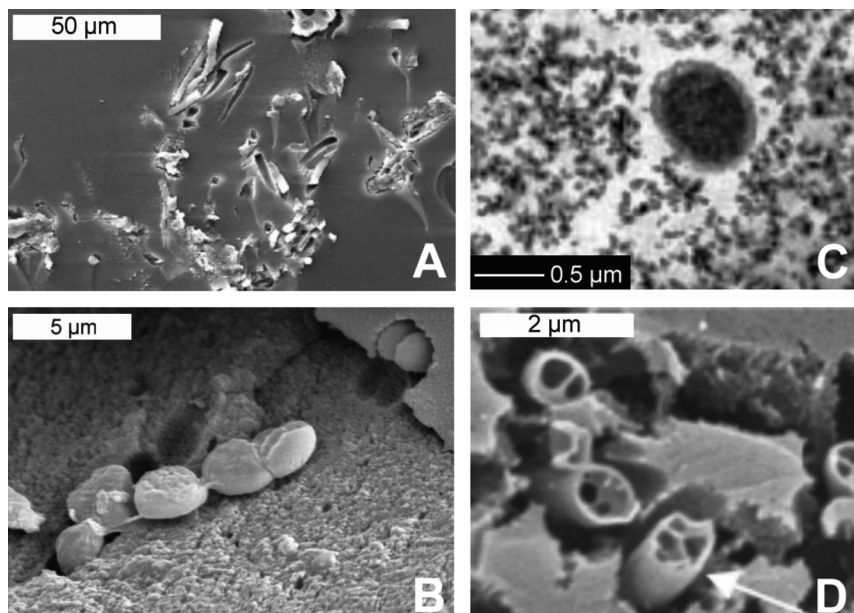


**Fig. 1.4** Scanning electron micrographs of (A) the lichen *Pseudocyphellaria hirsuta*, (B) the alga *Anabaena*, and (D) the bacteria *E. coli* entrapped in sol–gel generated organopolysiloxane matrices (reprinted with permission from [65]). (C) Transmission electron micrograph of the same bacteria, *E. coli*, embedded in a silica matrix containing 10 % glycerol (reproduced from [63] by permission of The Royal Society of Chemistry).

Copyright 2006, American Chemical Society.

One of the first works reporting the entrapment of *E. coli* proposed its incorporation in a TMOS-derived silica network in which the water content was kept at about 70 wt% in order to guarantee the cells' viability, but when silica gel was dried the bacterial activity decreased [62]. In order to overcome this drawback, the authors explored other possibilities such as the incorporation of glycerol in the silica matrix to increase bacteria viability (Figure 1.4C), leading to almost 50 % of viable bacteria after one month of ageing [63], or the addition of “quorum sensing” molecules involved in intercellular communication, which increase the cells' viability to 100 % after one month [64]. Similar results have been achieved recently by Ferrer *et al.* [65], who showed that gluconolactone-bearing organopolysiloxane matrices are more efficient than pure silica in extending *E. coli* the cells' viability due to their increased biocompatibility (Figure 1.4D).

New materials that mimic liposomes have been recently reported as a new family of organic–inorganic hybrid compounds generated by a coupled process of sol–gel and self-assembly of long-chain containing organoalkoxysilanes [18,66–71]. These nanohybrids essentially refer to biomimetic materials derived from the assembly of a surfactant covalently bonded to a silica-based network. The name “cerasomes” was introduced by Ariga and coworkers [66] combining the terms “liposome” and “ceramic,” this last making reference to the silica network. As “ceramic” is derived

from the Greek word κεραμικός (*keramikos*) making reference to “inorganic non-metallic materials whose formation is due to the action of heat” [72], the term cerasome can be confusing as they are usually formed in soft conditions. Ruiz-Hitzky suggests the use of HOILs (Hybrid Organic–Inorganic Liposomes) for this class of compounds [18]. Anyway, “cerosome” is actually the most popular term for these hybrid materials. Interestingly, the bilayers formed by the surfactant tails are able to incorporate different organophyllic species [71] making these materials potentially applicable as Drug Delivery Systems (DDS). More recently, these types of bilayers have been grafted onto magnetic nanoparticles giving rise to the so-called “magnetocerasomes” [73], which are nanohybrids simultaneously having lipophilic character and magnetic properties (see below, Section 5).

### 1.3

#### Calcium Phosphates and Carbonates in Bioinspired and Biomimetic Materials

As pointed out in Section 2, a wide number of biominerals are synthesized in nature by living organisms using organic templates. Some well-known examples include bone and ivory, where the collagen matrix controls the growth of hydroxyapatite (HAP) mineral [8,9,74], or nacre in pearls and shells, showing a brick-like structure of aragonite layers cemented by proteins [11,12]. This assortment of biological–inorganic hybrid materials, showing a hierarchical arrangement from the nano- to the macroscale, serves as a model for the development of new biomimetic and bioinspired materials. *In vitro* studies have demonstrated the controlled nucleation and growth of carbonates and phosphates by soluble proteins and peptides combined with insoluble polysaccharide matrices (cellulose, chitin, collagen), leading to biomimetic materials that reproduce the exceptional features of native biominerals [1,75].

Besides nacre in pearls and shells, calcium carbonate is also present in sea urchin spines, coral skeleton, eggshell, and the exoskeleton of arthropods, forming organic–inorganic hybrid structures by assembly with biomacromolecules (soluble proteins and insoluble matrices) [76–78]. Calcite and aragonite are the calcium carbonate polymorphs that constitute the biominerals found in nature, since they show a higher stability than vaterite. However, *in vitro* studies have confirmed that the presence of functionalised macromolecules as soluble proteins and insoluble matrices have a considerable effect on calcium carbonate crystallization, allowing the formation of the less stable polymorphs and even of amorphous  $\text{CaCO}_3$  [79,80]. Regarding soluble matrices, living organisms secrete biomacromolecules with a high content of glutamic and aspartic acids, bearing carboxyl groups that can interact with calcium ions. A similar effect has been found using polymers provided with sulfonic, hydroxy and even ether groups. Many of these studies have been carried out using the same biopolymers that act as insoluble matrices for  $\text{CaCO}_3$  crystallization in nature, such as collagen and chitin [79,81]. Calcium carbonate polymorphs are also formed on other natural and synthetic polymers including elastin that controls the formation of calcite [82], poly(ethylene glycol) that forces the selective formation of aragonite [83], poly( $\alpha$ -L-aspartate) that promotes vaterite formation with a helical morphology [84], or

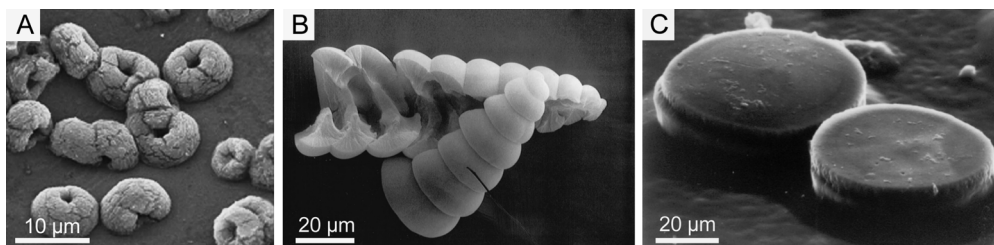


**Fig. 1.5** SEM micrographs of (A) donut-shaped CaCO<sub>3</sub> crystals grown on polyacrylic acid grafted chitosan, (B) CaCO<sub>3</sub> hollow helix, fractured by micro-manipulation, formed on poly( $\alpha$ -L-aspartate), and (C) double layered aragonite thin films grown on a chitosan matrix in the presence of poly(aspartate) and MgCl<sub>2</sub> by alternate spin coating and crystallization. (A) and (B) adapted from [84] and [85] with permission from Elsevier, and (C) from [88] (reproduced by permission of The Royal Society of Chemistry).

poly(acrylate)-grafted chitosan giving rise to CaCO<sub>3</sub> crystals of unusual morphology [85] similar to those created using poly(*N*-isopropylacrylamide-*co*-(4-vinylpyridine)) as the platform for mineralization [86]. As confirmed by these reports, materials scientists are able to produce calcium carbonate organic hybrid materials with defined morphologies (Figure 1.5) by tuning the polymers and biomacromolecules that control the nucleation and growth of calcium carbonate crystals. Many studies are currently centered on the crystallization of CaCO<sub>3</sub> as thin films, as illustrated in Figure 1.5C, trying to mimic the nacre of shells [87–89]. The reason is that mollusk shells, where the organic matrix constitutes only 1% of the total weight, present a fracture toughness about 3000 times higher than that of pristine calcium carbonate and offer a good example of ultra-lightweight hybrid materials with exceptional mechanical strength and interesting optical properties.

Calcium phosphate minerals are present in living organisms as the most important constituents of biological hard tissues (bones, teeth, tendons, and cartilage) to provide them with stability, hardness and function [74,90]. Among the different calcium phosphates, hydroxyapatite (HAP), with a chemical composition Ca<sub>10</sub>(PO<sub>4</sub>)<sub>6</sub>(OH)<sub>2</sub> and Ca/P ratio of 1.67, is the most widely studied due to its huge incidence in the field of regenerative medicine. Bone can be regarded as a natural nanocomposite containing HAP nanocrystallites in a collagen-rich matrix also enclosing non-collagenous proteins. Besides providing structural support, bone serves as a reservoir of calcium and phosphate ions involved in numerous metabolic functions. Due to the significant role of bone in humans, most of the synthetic hybrid materials that mimic its structure and composition are currently devoted to biomedical applications for regeneration of injured bone and this fact has led to a wide number of scientific publications on this topic in the recent years.

Among synthetic materials for bone grafting, nanocomposites are replacing metals, alloys, ceramics, polymers, and composites, due to their advantageous properties: large surface area, high surface reactivity, relatively strong interfacial bonding, flexibility, and enhanced mechanical consistency. It has been proved that nanocrystalline HAP offers better results than microcrystalline HAP with respect to osteoblast cells adhesion, differentiation and proliferation, as well as

biomineralization [74,91]. In addition to suitable mechanical properties, the requirements for these implants employed as a bioresorbable scaffold for bone regeneration are biocompatibility, suitable porosity with interconnected pores, as those observed in natural bone, to allow for the transport of nutrients and metabolic wastes, and controlled biodegradability, serving as a temporary scaffold for generation of new tissue [92,93].

Most of the bio-nanocomposites tested as implants for bone regeneration are based on the assembly of HAP nanoparticles with collagen, trying to reproduce the composition, biocompatibility and suitable mechanical properties of natural bone. The aim is to develop implants that mimic the nanostructuration, porosity and surface roughness of bone in order to facilitate the spreading of osteoblasts required for bone regeneration (Figure 1.6). Nanocrystalline HAP–collagen nanocomposites synthesized by biomimetic routes show a structure and composition very close to those of natural bone, providing better results in bone regeneration than nanocomposites prepared by conventional methods such as blending or mixing [94,95]. Murugan and Ramakrishna [74] have also reviewed the use of tissue-engineered nanocomposites, consisting in the isolation of specific cells by biopsy and their growth on a suitable nanocomposite scaffold, which is subsequently transplanted into the damaged bone site to promote its regeneration.

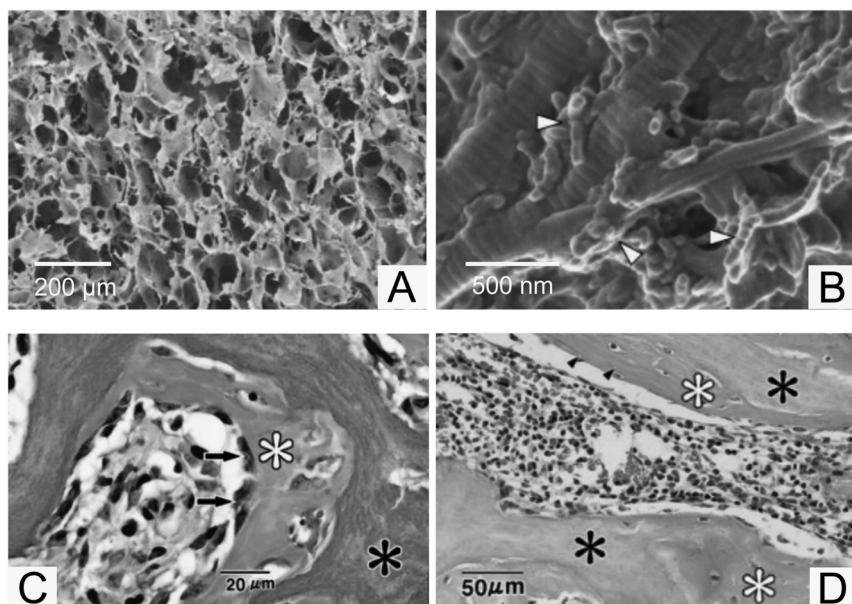


**Fig. 1.6** (A and B) Scanning electron micrographs of the porous hydroxyapatite–collagen nanocomposite scaffolds at different magnifications. Arrowheads in B indicate the hydroxyapatite nanocrystals on the collagen fibrils. Histology at (C) 1 week and (D) 4 weeks after

implantation in the bone marrow showing formation of new bone (white asterisk) attached directly to the nanocomposite (asterisk). Arrows indicate cuboidal osteoblasts on the surface of new bone. Adapted from [94], reproduced by permission of Wiley-VCH.

Besides the previously mentioned collagen, a wide variety of natural polymers have been involved in the synthesis of bio-nanohybrid materials with potential application in bone repair and dental prostheses. For instance, some recent examples refer to bio-nanocomposites based on the combination of HAP with alginate [96,97], chitosan [98,99], bovine serum albumin (BSA) [100], sodium caseinate [101], hyaluronic acid [102], silk fibroin [103,104], silk sericin [105], or polylactic acid (PLA) [106,107]. These examples illustrate the increasing interest in the subject of HAP-based biohybrid materials, which has led to almost 400 articles appeared in scientific journals in 2006 alone.

Given that macroporosity is an important requirement for materials used as implants in regenerative medicine, many of the developed HAP-based materials try to mimic not only the composition but also the porous structure of true bone. For this reason, different techniques such as fiber bonding, phase separation, solvent casting/particle leaching, gas foaming, and emulsification/freeze-drying, are being tested to create superporous matrices with interconnected pores [92,108]. A bioinspired procedure has been followed by Deville *et al.* [109] consisting in the directional freezing of an HAP suspension. This technique produces an arrangement of HAP in well defined layers due to the growth of ice, resulting in a multilayered structure that resembles nacre.

Bio-nanocomposites based on calcium phosphates can perform other innovative functions such as acting as a reservoir for the controlled release of bioactive compounds once the material is implanted in the bone defect. For instance, the incorporation of a morphogenetic protein that promotes bone regeneration in an HAP–alginate–collagen system [110] or a vitamin in a Ca-deficient HAP–chitosan nanocomposite [111] are recent examples of this kind of application.

In addition to hydroxyapatite, other calcium phosphate minerals such as tricalcium phosphate (TCP), substituted apatites, as well as cements and biphasic mixtures with calcium phosphate content have also been studied for clinical applications, as extensively reviewed by Vallet-Regí and González-Calbet [112]. Although to a lesser extent than hydroxyapatite-based analogues, several biohybrid materials based on tricalcium phosphate (TCP,  $\text{Ca}_3(\text{PO}_4)_2$  with  $\text{Ca}/\text{P} = 1.50$ ) have been reported in the last few years. Some representative examples refer to microcomposites involving  $\beta$ -TCP in combination with structural proteins, polysaccharides or biodegradable polyesters such as collagen [113], chitosan [114] and PLA [115]. Calcium phosphate cements are also used as scaffolds for bone regeneration due to their biocompatibility, being gradually replaced by new bone after implantation. Their assembly with biopolymers results in highly stable biocomposites in which adhesion, proliferation and viability of osteoblasts are enhanced. This is the case of biocomposites based on chitosan combined with tetracalcium phosphate (TTCP,  $\text{Ca}_4(\text{PO}_4)_2\text{O}$ ) and dicalcium phosphate anhydrous (DCPA,  $\text{CaHPO}_4$ ) applied in periodontal and bone repair [116,117]. Among substituted apatites, fluorapatite is being studied as a component of hierarchically grown gelatin-based bio-nanocomposites showing a fractal character (Figure 1.7). The material synthesized by biomimetic routes has a composition very close to that of mature tooth enamel, with the formula  $\text{Ca}_{5-x/2}(\text{PO}_4)_{3-x}(\text{HPO}_4)_x(\text{F}_{1-y}(\text{OH})_y) \cdot 2.3 \text{ wt\%}$  gelatin ( $x = 0.82$ ;  $0 < y \leq 0.1$ ), showing potential application in dentino- and osteogenesis [118,119].

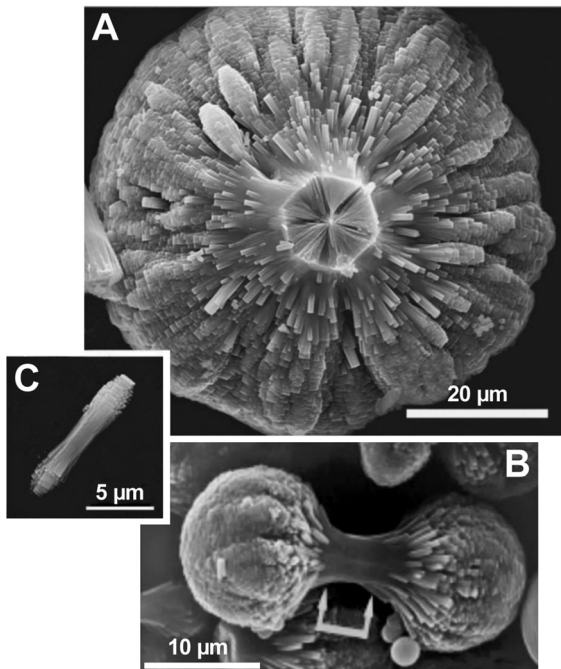


**Fig. 1.7** Scanning electron micrographs showing fractal pattern formation by hierarchical growth of fluorapatite–gelatin nanocomposites: (A) half of a dumbbell aggregate viewed along the central seed axis, (B) dumbbell aggregate at an intermediate growth state, and (C) central seed exhibiting tendencies of splitting at both ends (“small” dumbbell). Adapted from [119], reproduced by permission of Wiley-VCH.

## 1.4

### Clay Minerals and Organoclay Bio-nanocomposites

In Earth, besides phosphates and carbonates, one of the most abundant groups of inorganic solids in interaction with the Biosphere is represented by the family of the so-called clay minerals [120]. They are silicates of aluminum and/or magnesium structured in tetrahedral and octahedral environments arranged as sheets that share oxygen atoms. Clay minerals showing two types of morphology have been used for the preparation of bio-nanocomposites: layered and microfibrous silicates. The first group includes montmorillonite, which is an aluminosilicate belonging to the smectite minerals group that show cation-exchange and expandability properties. The second group is represented by sepiolite, a microfibrous hydrated magnesium silicate whose main characteristics are determined by its textural behavior and surface reactivity.

Smectites are 2:1 charged layered silicates from natural (montmorillonite, hectorite, beidellite, saponite etc.) or synthetic (synthetic fluorohectorites, such as

Laponite) origin, built up by two tetrahedral silica sheets sandwiching one Al/Mg octahedral central sheet. In montmorillonite, the octahedral sheet is built up from  $\text{Al}^{3+}$  ions partially replaced by other cations such as  $\text{Fe}^{3+}$  and  $\text{Mg}^{2+}$ . The presence of divalent cations in that sheet and, to a lesser extent,  $\text{Al}^{3+}$  in the tetrahedral sheets, generates a negative charge compensated by extra-framework cations that are usually located as hydrated species in the interlayer region of the silicate [120]. Natural smectites are hydrophilic materials in which the accessibility of water to the interlayer region determines their colloidal properties, leading to gelatinous and viscous fluids and favoring its combination with water-soluble biomolecules. This is particularly significant for smectites containing alkaline ions in the interlayer region that may induce the swelling of the clay in water, promoting delaminated systems that allow their combination with molecular and macromolecular species, resulting in nanostructured system formation, including biopolymer-clay nanocomposites (bio-nanocomposites) [121–123].

Saccharides such as sucrose easily intercalate montmorillonite from aqueous solutions [124] giving basal spacing values of 1.64 and 1.83 nm [125], respectively, ascribed to mono- or bi-layer molecular arrangements in the interlayer space of the clay mineral. Recently, the intercalation of sucrose and its further *in situ* polymerization activated by microwave irradiation appears as a new procedure for the preparation of the bio-nanocomposites called caramel-clay nanostructured materials [126]. In this case, the bio-nanocomposite shows a value of about 1.9 nm corresponding to the intercalated caramel, which is characterized by chemical analyses, FTIR and  $^{13}\text{C}$ -NMR spectroscopies [126]. These bio-nanocomposites act as precursors for the carbon-clay nanocomposite formation giving rise to electrical conductor solids. The starting caramel-montmorillonite is an insulating material that increases in conductivity ( $\sigma$ ) from  $\sigma < 10^{-12}$  S/cm to  $\sigma \approx 0.1$  S/cm after the carbonization process. The most salient feature reported for these carbonaceous nanostructured materials is the combination of their electrical and textural behaviors suitable for potential applications as electrodes for electroanalysis, electrocatalysis, and in energy storage (supercapacitors) devices [127]. In this context, it must be taken into account that these materials are prepared from natural resources, therefore being considered as low cost environmentally friendly functional materials. This type of carbonaceous material is also formed by the direct pyrolysis of the carbohydrate-clay system containing small amounts of sulfuric acid [128].

Positively charged polysaccharides act as polyelectrolytes, being able to intercalate montmorillonite and other smectites by ion-exchange reactions from solutions [3]. By controlling the equilibrium concentration of chitosan in diluted acetic acid, it is possible to control the access of the biopolymer to the interlayer space of montmorillonite, leading to bio-nanocomposites with one, two or even more layers of intercalated polymer [129,130]. The incorporation of chitosan as a monolayer is governed by the cation-exchange capacity (CEC) of montmorillonite (about 90 mEq/100 g), whereas larger amounts of the polysaccharide, exceeding the CEC, lead to multilayer configurations. This last arrangement takes place by ion-exchange incorporation of chitosan aggregates formed in the concentrated solutions, which are self-assembled through hydrogen bonding, the charge excess being compensated with

acetate anions. In this manner, these counter-ions are entrapped in the interlayer space and, therefore, the resulting bio-nanocomposites show anionic exchange properties, as confirmed by various techniques including  $^{13}\text{C}$  NMR solid-state studies [130]. Intercalation of chitosan in Na-montmorillonite using solutions containing a high biopolymer/clay ratio may produce exfoliation of the layer silicate, in agreement with XRD and TEM results [131]. By solvent casting, these exfoliated materials have good film-forming ability, showing enhancement of the tensile strength and a decrease in the elongation-at-break compared to chitosan without montmorillonite. This behavior opens the way to new applications towards development of the so-called *green nanocomposites* (bioplastics) with potential applications in tissue engineering and food packaging.

Chitosan–clay bio-nanocomposites are very stable materials without significant desorption of the biopolymer when they are treated with aqueous salt solutions for long periods of time. In this way, they act as active phases of electrochemical sensors for detection of ions (Figure 1.8). The particular nanostructuration of the biopolymer in the interlayer region drives the selective uptake of monovalent versus polyvalent anions, which has been applied in electrode arrays of electronic tongues [132].

Chitosan–clay bio-nanocomposites showing the ability to incorporate anionic species can be used to prepare functionalized biohybrids. An example is the uptake of anionic dyes such as fast green and naphthol yellow S which are low-toxicity

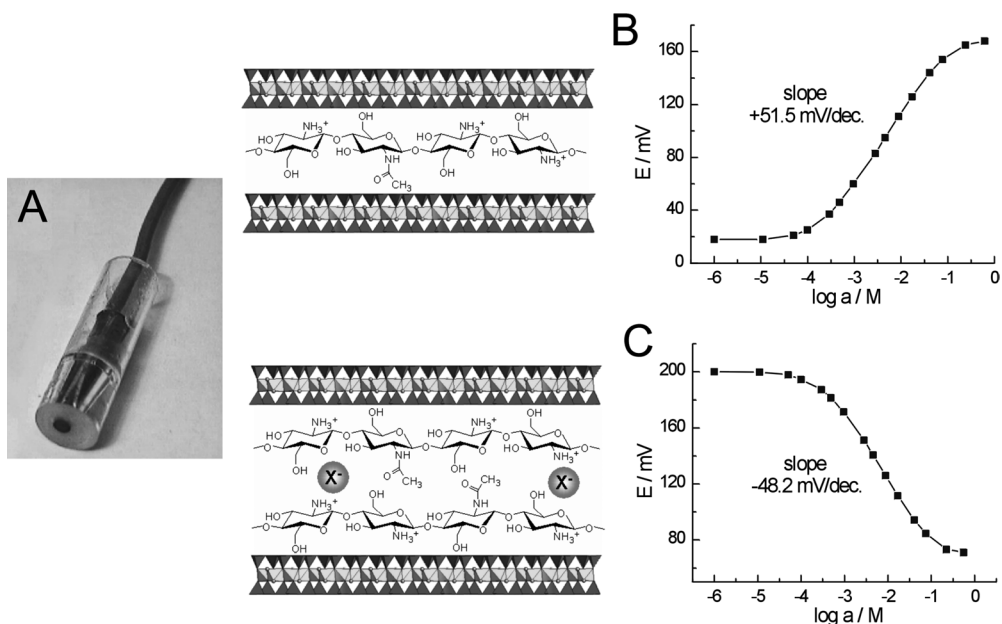


**Fig. 1.8** (A) Design of a chitosan-montmorillonite sensor. Arrangement of chitosan chains in the clay interlayer space as a monolayer (B) or a bilayer (C) resulting in opposite behavior when measuring NaCl solutions of increasing concentration by direct potentiometry.

compounds even used as additives in food and cosmetics [133]. Interestingly, these dye/chitosan–clay hybrids are being used in applications as non-cytotoxic photo-protector systems providing considerable photostabilization of entomopathogenic fungus such as the conidia of *Aschersoni*. spp., which is used as a model biocontrol agent. In this context, assuming that the chitosan–clay bio-nanocomposites are biocompatible materials and also show capacity to absorb ionic species, they could, potentially, be used as vectors for controlled drug delivery of anionic drugs.

As chitosan is an excellent adsorbent for organic compounds its assembly with clay minerals could be interesting with regard to enhancing its mechanical properties for practical uses. Chang and Juang [134] have prepared composite beads by combination of activated clay and chitosan, developing adsorbents for dyes and organic acids (tannic and humic acids). Chitosan–clay biohybrids can be useful as intermediates for nanocomposites as they incorporate chemical functionality into the inorganic substrates. Qiu *et al.* [135] reported that monomers, such as acrylic acid, can react with these biohybrids producing their immobilization. Further polymerization gives rise to improved photostable polyacrylic acid/chitosan–clay nanocomposites, which exhibit water-superabsorbent properties.

The ion-exchanging ability of smectite clay minerals allows the development of intercalation compounds by treatment with salt solutions of organic cations, such as long-chain alkylammonium ions giving the so-called organoclays materials [121,122,136]. Organoclays show a better affinity towards non-polar species, which in this way may be assembled to the internal and the external surfaces of the modified clay mineral. Various authors have reported the preparation of bio-nanohybrid materials based on organoclays [137–144]. As this topic is specifically treated in Chapter 8, we will refer to it briefly here with some examples. Probably the most popular biohybrids are the poly L-lactic acid (PLA)–organoclay composites, usually prepared by a melt intercalation process [137,142,143,145]. These bio-nanocomposites (Figure 1.9A) show improved characteristics with respect to neat PLA, such as thermomechanical and gas barrier properties. This improvement, together with the PLA biodegradability behavior, makes these reinforced PLA bioplastics excellent

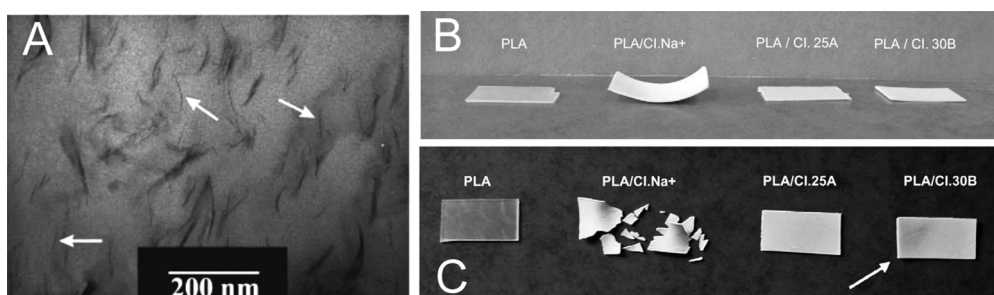


**Fig. 1.9** (A) Exfoliation of clay platelets (white arrows) in a commercial polylactide matrix using a “masterbatch” process. (B, C) Visual aspect of unfilled PLA, microcomposite based on Cloisite $\text{Na}^+$ , and nanocomposites based on

Cloisite25A and Cloisite30B after (B) two and a half months hydrolysis and (C) after five and a half months hydrolysis. (A) adapted from [144] reproduced by permission of Wiley-VCH, and (B, C) from [147] with permission from Elsevier.

candidates for applications in the food industry and for biomedical purposes. It is important to signal that the biodegradability of these bio-nanocomposites strongly depends on the nature of the organoclay used as nanofiller [4,146,147]. In fact, the use of natural unmodified montmorillonite results in the formation of microcomposites that undergo fast degradation in comparison to nanocomposites formed from organomontmorillonites (Figure 1.9B, C). However, the incorporation of organoclays in bio-nanocomposites by assembly with biopolymers is not always advantageous for improving the final properties of the resulting biohybrids. This is, for instance, the case with chitosan-Cloisite 30B nanocomposites in which mechanical and thermal properties get worse in comparison with analogous bio-nanocomposites prepared from  $\text{Na}^+$ -exchanged montmorillonite [131]. This apparently contradictory behavior points out the importance of both the relative hydrophilicity of the clay layers and the nature of the biopolymer in the characteristics of the resulting nanocomposite and its final properties.

On the other hand, we have signaled (see above) the role of microfibrous clay minerals (sepiolite and palygorskite) in developing new nanocomposites. Sepiolite is structurally arranged by blocks formed by an octahedral sheet of magnesium oxide/hydroxide packed between two tetrahedral silica layers [148,149]. The periodic inversion of the  $\text{SiO}_4$  tetrahedra determines a regular discontinuity of the sheets, being the origin of the structural cavities (*tunnels*) extended along the *c* axis, that is the axis of the microfibers [148] and the presence of silanol groups ( $\text{Si}-\text{OH}$ ) [150,151]. Sepiolite shows a lower CEC than smectites ( $\sim 15$  compared to  $\sim 100$  mEq/100 g) but, in addition to acting as an ion-exchanger able to uptake charged biopolymers, the presence of silanol groups on its external surface favors its association through hydrogen bonds. This last mechanism of interaction has been invoked to explain the formation of bio-composites with structural proteins (e.g., collagen) and polysaccharides (e.g., chitosan) via the amino and hydroxy groups of the respective biopolymers [152]. In the case of the fibrous proteins such as collagen, the interaction results in an exceptional arrangement of the biopolymer oriented in the same direction as the sepiolite fibers [34]. Further incorporation of low amounts ( $< 1\%$ ) of glutaraldehyde confers to the collagen–sepiolite biohybrids a strong improvement in mechanical properties, with excellent persistence after several months of implantation for bone repair applied to *in vivo* assays [33].

Chitosan shows high affinity for sepiolite assembly as, in addition to the hydrogen bonding between  $\text{Si}-\text{OH}$  surface groups and the biopolymer hydroxy groups, the negatively charged surface of the silicate could be balanced by the protonated amino groups of the biopolymer [3,31]. Multilayer coverage of chitosan can take place at high equilibrium concentrations of chitosan, which is adsorbed as polymer aggregates, similarly to chitosan–smectite interactions (see above). Sepiolite becomes strongly integrated within the biopolymer structure (Figure 1.10A), in a similar way to the chitosan–montmorillonite material (Figure 1.10B), providing nanohybrids that show good mechanical properties. In this way, the elasticity modulus of these bio-nanocomposites is superior to those of the components measured separately, which is the typical synergistic effect reported for structural polymer–clay nanocomposites [31]. Alternatively, sepiolite bio-nanocomposites have been used as precursors

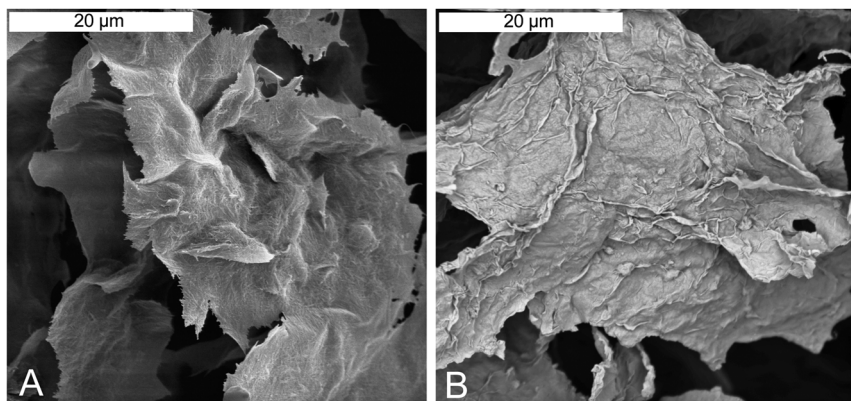


**Fig. 1.10** SEM micrographs of chitosan-based bio-nanocomposites involving (A) sepiolite and (B) montmorillonite as the inorganic moiety.

of multifunctional materials, as reported by Gómez-Avilés *et al.* [153]. In this case, a precursor caramel-sepiolite bio-nanocomposite, prepared by application of MW irradiation to sucrose–sepiolite mixtures, can be turned into the corresponding carbonaceous derivative after pyrolysis at 800 °C in a N<sub>2</sub> atmosphere. These materials show significant electronic conductivity and, interestingly, they can be further functionalized by reaction with organosilanes. Grafting of aminopropyltrimethoxysilane and subsequent protonation of the amino groups, results in a material that can act simultaneously as an electronic collector and a sensing phase when used as an electrochemical sensor for anion detection. It is able to discriminate anions by their size and charge due to its textural behavior [153].

The structure and morphology of palygorskite are strongly related to those of sepiolite, although it shows higher Al content and narrower tunnels [120]. This microfibrous silicate acts similarly to sepiolite, assembling biopolymers via hydrogen bonding. In this way, hydroxyethyl and hydroxypropyl cellulose associate to palygorskite modifying the rheological behavior of the clay dispersions [154]. Palygorskite can also be combined with modified polysaccharides, such as polyacrylamide (PAA) grafted-starch, giving rise to bio-nanohybrids with extraordinary superabsorbent properties as they may absorb up to 500 g of water per g of bio-nanocomposite [155].

Layered Double Hydroxides (LDHs), also called *hydrotalcite-like materials* or even *anionic clays*, are mixed hydroxides that can be described by the general formula  $[M^{2+}_{1-x}M^{3+}_x(OH)_2][A^{n-}_{x/n} \cdot zH_2O]$  in which M<sup>2+</sup> and M<sup>3+</sup> are metal ions and A<sup>n-</sup> is the anion that compensates the deficit of negative charge in the layers. In contrast to the above-mentioned smectite clay minerals, the main characteristics of LDHs are the high charge density in the layers and the anion exchange ability. In this way, LDHs can be assembled with negatively charged biopolymers leading to biohybrids equivalent to those prepared from smectites, often showing intercalated or partially delaminated phases. An example of this type of bio-nanocomposite is the Zn-Al LDH assembly with negatively charged polysaccharides (alginate, pectin,

$\kappa$ -carrageenan and  $\iota$ -carrageenan) [156,157]. These biohybrids are prepared by the so-called template synthesis of the LDH inorganic host in the presence of the biopolymer. The self-assembly of the polysaccharide in the medium in which the LDH is synthesized determines the incorporation of biopolymer aggregates, in which a part of the electrical charge is compensated by the LDH host and the other moiety by extra-framework cations. This situation is the inverse to that reported for chitosan–smectite bio-nanocomposites and is the basis for their application as active phases of potentiometric sensors. In this way, potentiometric sensors for calcium ions have been developed, profiting from the ability of the biopolymers alginate,  $\iota$ -carrageenan, pectin and  $\kappa$ -carrageenan to complex calcium ions [157]. The comparative study demonstrates that sensors based on the two last bio-nanocomposites show a lower sensitivity in the determination of  $\text{Ca}^{2+}$  ions, probably due to the complex structure of pectin and to the low content of negatively charged groups in the  $\kappa$ -carrageenan chains with respect to the other polysaccharides.

The ability of LDHs to interact with negatively charged biopolymers has been applied to the preparation of biohybrid materials incorporating negatively charged DNA in Mg-Al LDH, as firstly reported by Choy and coworkers [158–160]. These bio-nanohybrids exhibit the unique property of acting as non-viral vectors in gene therapy to transfer nucleic acids to the cell interior via an endocytosis mechanism (Figure 1.11A). LDH-based biohybrids can also be used as carriers for controlled drug delivery, as diverse bioactive compounds are negatively charged [3]. LDHs can also be assembled with enzymes producing their effective immobilization between the inorganic layers, whilst at the same time allowing the diffusion of substrates and products (Figure 1.11B). An illustrative example is the entrapping of urease within Zn-Al LDH giving rise to bio-nanohybrids able to act as active phases in capacitance biosensors [161]. This topic will be more deeply considered in Chapter 15.

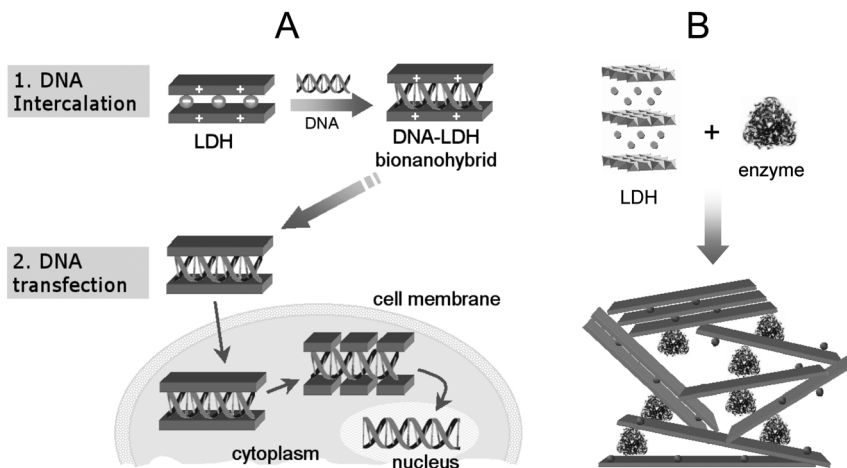


**Fig. 1.11** Applications of LDHs as (A) non-viral vector in gene therapy for transfection of DNA to the cell nucleus, and (B) as matrix for enzymes immobilization in the development of biosensors.

## 1.5

## Bio-Nanohybrids Based on Metal and Metal Oxide Nanoparticles

The dispersion of metallic, semiconductor or magnetic nanoparticles in polymeric matrices results in easy-handling nanocomposite materials that can be used in a wide number of applications. Nowadays, the use of biopolymers for this purpose is increasing since they are an eco-friendly alternative to the usually employed polymers, mainly for applications in the health area. For instance, bio-nanocomposites based on silver oxide nanoparticles have been prepared by embedding them in a gelatin matrix. This new bio-nanohybrid material shows luminescent intensity higher than non-modified nanoparticles after activation with a femtosecond-laser. This feature, together with the appropriate mechanical properties of the gelatin- $\text{Ag}_2\text{O}$  nanoparticles nanocomposite, makes possible its application in light-emitting materials for all-optical logic devices or data-storage media [162].

The branched polysaccharide dextran is assembled with alkanethiol-modified gold nanoparticles and the resulting nanocomposite is then functionalized to facilitate the specific binding of target biomolecules. This biorecognition process can be easily detected by particle plasmon resonance (PPR), based on the optical properties of gold nanoparticles [163].

Charged polysaccharides can also serve as templates for the growth of metallic, semiconductor and magnetic nanoparticles. For instance, chitosan has been reported as a catalyst and stabilizing agent in the production of gold nanoparticles by the reduction of tetrachloroauric (III) acid by acetic acid. The biopolymer controls the size and the distribution of the synthesized Au nanoparticles and allows the preparation

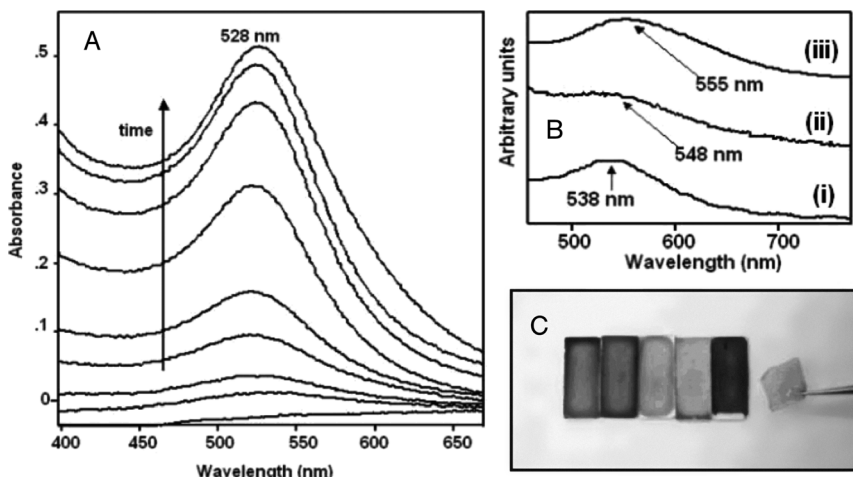


**Fig. 1.12** (A) Increase in surface plasmon absorption as Au nanoparticles are produced from a reaction mixture containing 1% chitosan, 1% acetic acid and 0.01% tetrachloroauric (III) acid ( $\text{HAuCl}_4$ ); (B) shift of surface plasmon absorption and from mixtures with lower chitosan concentration (ii) or lower  $\text{HAuCl}_4$  amount (iii); six different self-sustained nanocomposite films showing the control over the optical properties. Reprinted with permission from [164], 2004, American Chemical Society.

of self-supported gold–chitosan bio-nanocomposite films (Figure 1.12). This bio-nanohybrid material shows potential application in the development of biosensors and in trace chemical analysis [164]. The same polysaccharide, chitosan, is involved in a new CdS quantum dots–chitosan bio-nanocomposite. In this case, the ability of chitosan to complex transition metal ions is used to entrap Cd<sup>2+</sup>, followed by immersion of the resulting Cd<sup>2+</sup>–chitosan films in Na<sub>2</sub>S solution to yield the CdS semiconductor nanoparticles. The size of the formed quantum dots is limited by the polysaccharide, which also avoids agglomeration of the nanoparticles. The resulting bio-nanocomposites exhibit increased thermal stability and improved aqueous solubility [165]. A similar procedure was followed with the anionic polysaccharide alginate, used as template for the controlled growth of Ni, Co or NiCo magnetic nanoparticles. In this case, the nanocomposites are processed as microcapsules resulting from gelation of alginate in the presence of Ni<sup>2+</sup>, Co<sup>2+</sup> or a mixture of both ions, which are further reduced under H<sub>2</sub>/N<sub>2</sub> flow [166]. A recent contribution by Srivastava *et al.* [167] reports the formation of magnetic bio-nanocomposites by assembly of cationic FePt nanoparticles and DNA.

On the other hand, metal oxide nanoparticles such as Al<sub>2</sub>O<sub>3</sub>–Zr<sub>2</sub>O have been used recently to reinforce biological matrices such as collagen, enhancing their mechanical and thermal properties and leading to hybrid materials with potential use in biomedical and bionic applications [168]. Of particular interest for such types of applications, including NMR imaging, hyperthermia treatment, and targeted drug delivery, is the use of nanoparticles based on metal oxides showing magnetic properties [169,170]. Ferrites (magnetite or maghemite) prepared as nano- or micro-particles [29,171] become biocompatible after assembly with biopolymers (poly-DL-lactate, starch, pectin, alginate) or biocompatible polymers (poly-acrylates, polyvinyl alcohol) [172–174]. Magnetic bio-nanocomposites from the assembly of magnetic nanoparticles and fibers of biopolymers such as poly(hydroxyethylmethacrylate) (PHEMA) or PLA have been prepared recently by the electrospinning technique [175]. This type of material was developed for accumulation of delivered drugs in a precise target area, due to its superparamagnetic properties and its ability to release the transported drug. Bio-nanocomposites based on dextran and magnetic nanoparticles such as magnetite or maghemite have been described as physiologically well-tolerated materials [28], being studied for use in different biomedical applications [29].

Alternatively, magnetic nanoparticles can be incorporated within a bilayer of phospholipids arranged as a liposome (Figure 1.13A). These systems, called magnetic liposomes or magnetoliposomes, were developed with the aim of entrapping and transport molecular species or genetic matter acting in DDS under the guidance of a magnetic field [176,177]. We have indicated above the interest in functionalizing magnetic oxide nanoparticles in the preparation of magnetocerasomes (see above, Section 2) by grafting long-chain cationic surfactants onto magnetite through silane or phosphonic moieties, which are further co-assembled with phosphatidylcholine (PC) (Figure 1.13B). In this context, magnetocerasomes show the ability to incorporate lipophilic target species, transporting them through artificial membranes being useful for the design of new carriers for DDS [73].

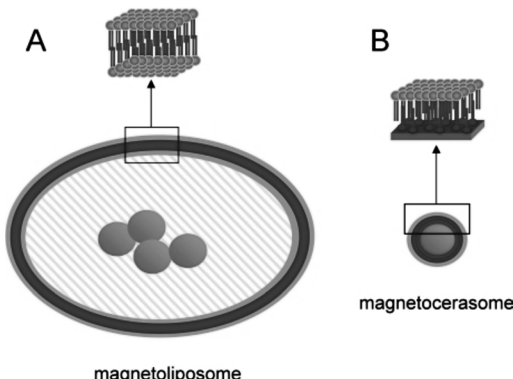


**Fig. 1.13** Schematic representations of (A) magnetoliposome and (B) magnetocerasome configurations involving magnetic nanoparticles and phosphatidylcholine.

Nanoparticles of  $\text{TiO}_2$  can be combined with biomolecules of different nature giving functional bio-nanocomposites. For instance, lysozyme has been encapsulated within titania nanoparticles resulting in nanohybrids showing antimicrobial activity. Here again, it is postulated that the inorganic moiety protects the enzyme against denaturation [178]. Moreover, bacterial immobilization on a nanocrystalline  $\text{TiO}_2$  matrix allows the development of bio-nanocomposites acting as the active phase of photoelectrodes [179]. This is an excellent example of how nanoparticles associated with biomolecules act not only as a mechanical support but also may confer functional properties to the bio-nanocomposite materials. In relation to this type of material, organically modified layered titanates were assembled with PLA to prepare *green nanocomposites* with improved mechanical properties. The photodegradation of PLA in sunshine is enhanced by the presence of the inorganic component, as the titanate shows photocatalytic activity similar to that of  $\text{TiO}_2$  [180].

Another semiconductor oxide such as  $\text{ZnO}$  is particularly promising in nanodevice applications. A pioneering work refers to the preparation of biofunctional  $\text{ZnO}$  nanorod arrays grown on a thermoplastic polyurethane flexible substrate and further assembled with proteins [181]. This innovative approach aims to develop new biological sensing systems showing flexible properties and biocompatibility, which are useful for the detection of complementary biomolecules on the acceptor side, such as antibody–antigen bioconjugation by photoluminescence spectroscopy [181].

## 1.6

### Carbon-based Bio-nanohybrids

Carbon nanotubes (CNTs) were discovered in 1991 by Iijima [182] and since then they have attracted much attention in many research fields. CNTs can be described as tubular structures rolled up from a graphene sheet. Depending on the number of tubular walls CNTs can be classified as single-walled carbon nanotubes (SWCNTs)

that show diameters in the range 0.7–1.5 nm, and multi-walled carbon nanotubes (MWCNTs), which are formed by 2–30 concentric tubes with diameters in the 2–10 nm for the inner tubular layer and additional thickness of about 0.7 nm for every additional layer [183]. Differences in the chiral vectors that describe how graphene sheets are rolled up, as well as topological defects present on the tube surface, determine the distinct electronic structures and therefore either the semiconducting or metallic behavior of CNTs. Besides their electrical properties, CNTs show exceptional mechanical properties due to their very high aspect ratio, which has made them very attractive for applications as nanofillers of different polymers [184–187].

Due to the poor solubility of CNTs in water, they are very frequently submitted to treatments with mixtures of concentrated sulfuric and nitric acids, which result in the formation of carboxyl and hydroxyl groups on their surface. Besides solubility in polar solvents, these activated CNTs are able to react with other functional groups favoring coupling to different compounds. In this way, chitosan–MWCNTs bio-nanocomposites have been prepared by a simple solution–evaporation method from activated CNTs, in order to favor their interaction with the amino groups of chitosan. The homogeneous distribution of MWCNTs in the biopolymer determines a significant improvement in the mechanical properties with 93 and 98 % enhancement in the tensile modulus and strength, respectively, with only a 0.8 %wt MWCNTs content [188]. The use of CNTs previously grafted to chitosan that are further blended to pure chitosan allows the incorporation of larger amounts of nanotubes, up to 50 %wt CNTs [189]. As compared with ungrafted CNTs, chitosan-grafted-CNTs show improved dispersion ability in the chitosan matrix, which results in significantly improved storage modulus and water stability. Spinks and coworkers [190] prepared SWCNTs–chitosan fibers confirming that improved dispersion of CNTs in chitosan results in enhanced mechanical properties without compromising swelling behavior. These materials also show pH actuation according to the variable pH swelling response, which makes them attractive for applications as bioactuators and artificial muscle materials.

The combination of CNTs and carbohydrates is also a research area of interest with regard to preparing bio-nanocomposites for biological applications. Thus, the preparation of multivalent carbohydrate–CNTs conjugates based on lactose-attached schizophyllan [191], lipid-terminated sugar polymers [192], and covalently attached sugar polymers [193,194] has been reported. In this way, *p*-N-acryloamidophenyl  $\alpha$ -D-glucopyranoside has been assembled with SWCNTs (Figure 1.14A) with the aim being to create materials able to show specific interaction with carbohydrate recognition proteins, which can be of interest for the recognition of bacterial toxins and viral proteins, or quantitative estimation of carbohydrate–carbohydrate interactions [195]. Functionalization of SWCNTs via atom transfer radical polymerization (Figure 1.14B) allows the direct grafting of sugar- and phosphorylcholine-based biopolymers, making the modified CNTs water soluble and biocompatible [35]. Interestingly, the resulting bio-nanocomposites based on the anchorage of the sugar moiety may have interest in carbohydrate–protein recognition, whereas the phosphorylcholine derivative could prevent nonspecific protein adsorption and cellular adhesion.

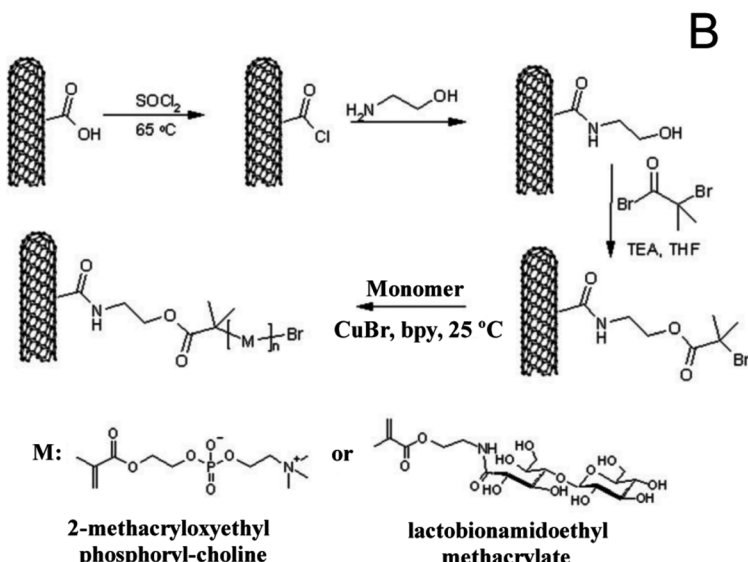
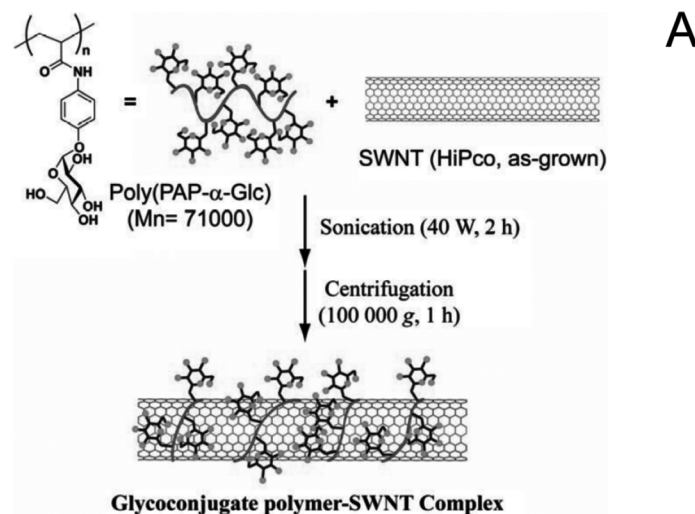


**Fig. 1.14** (A) Single-wall carbon nanotubes wrapped by glycoconjugate polymer with bioactive sugars. (B) Modification of carboxyl-functionalized single-walled carbon nanotubes with biocompatible, water-soluble phosphorylcholine and sugar-based polymers. (A) adapted from [195] with permission from Elsevier, and (B) from [35] reproduced by permission of Wiley-VCH.

An illustrative example of carbohydrate–protein recognition has been reported by Chen and coworkers [192] using a C18-mucin mimic polymer that interacts hydrophobically with SWCNTs. This biohybrid is able to specifically recognize the lectin *Helix pomatia* agglutinin (Figure 1.15A). Galactose-modified CNTs are able to capture

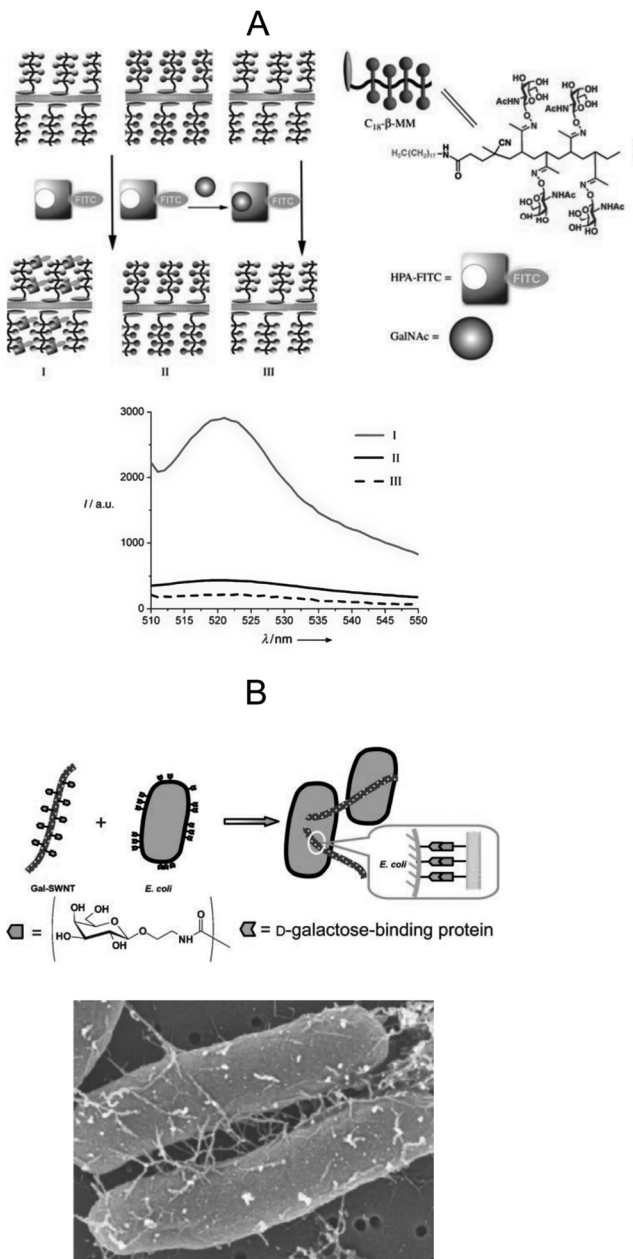


**Fig. 1.15** (A) Scheme for (I) specific binding of the lectin *Helix pomatia* agglutinin (HPA) to C18- $\alpha$ -MM-coated SWNTs, (II) lack of binding of HPA to C18- $\beta$ -MM-SWNTs, and (III) inhibition of HPA-binding by soluble GalNAc, as well as the corresponding fluorescence spectra (510–550 nm, excitation wavelength 492 nm). (B) Schematic

representation and SEM image showing the specific binding of galactose modified-SWNTs to galactose-binding proteins in *E. coli* cells. (A) Adapted from [192] (reproduced by permission of Wiley-VCH) and (B) from [194] (reproduced by permission of The Royal Society of Chemistry).

pathogens, for example *E. coli*, following a similar type of specific binding reaction (Figure 1.15B) [194]. Other biopolymers, such as DNA, have also been combined with CNTs to create bio-nanocomposites that can serve for instance as biological transporters and near-infrared agents for selective cancer cell destruction [196]. In relation to this application, it is important to signal that recent studies demonstrate that CNTs can cause DNA destabilization and conformational transition that are sequence-dependent [197].

Taking into account their electrical and mechanical properties, CNTs have been extensively investigated, not only as additives in the preparation of conventional bio-nanocomposites, but also in the development of biohybrids for various biomedical applications, including tissue regeneration, biosensors and other biomedical devices such as microcatheters [198]. For these types of application, a key point is their biocompatibility [199], as the presence of metallic compounds from the catalysts used in their synthesis introduces significant toxicity [200]. In this way, Koyama and coworkers have performed systematic studies on the biological response of CNTs used as microcatheters by measuring CD4<sup>+</sup> and CD8<sup>+</sup> T-cells in *in vivo* experiments, confirming their almost inert behavior in high-purity microcatheters [198]. These authors also indicate that several obstacles besides the use of defect-free and high-purity CNTs must be solved before their use in biomedicine is completely safe. These requirements include the preparation of biohybrids with a homogeneous dispersion of CNTs in polymers, control of the CNTs chirality, and long-term systematic biological studies of the materials. In this line of research, bio-nanocomposites from MWCNTs and poly(L-lactide), a polymer susceptible to enzymatic and hydrolytic degradation to L-lactic acid, have been prepared with the aim being to obtain a new generation of implant materials. Studies on related polylactic-*co*-glycolic acid combined with CNTs and poly(vinyl alcohol) suggest an important influence of the distribution of components on the surface of the material on its biocompatibility properties [201]. Other CNT-biocompatible polymer systems that have been explored with the aim of developing scaffolds for tissue regeneration applications are SWCNTs–poly(propylene fumarate) biohybrids [202]. These bio-nanocomposite systems show improved mechanical properties and good electrical properties that could be of interest in stimulating cell growth and tissue regeneration by facilitating the physioelectrical signal transfer. However, cell culture tests suggest that the presence of MWCNTs in the nanocomposites inhibits the growth of fibroblast cells [203].

The interesting electrical conductivity properties of CNTs have been used to develop different types of biosensors. Strategies to prepare these devices include for instance the use of layer-by-layer techniques to build the active phase on an electrode by entrapping an enzyme, such as glucose oxidase (GOD), within the CNTs layer [204,205]. The entrapping by electrostatic interactions seems to be preferable to the formation of true covalent bonding of CNTs, not only to preserve the activity of the protein but also to avoid variation in the conductive response of the active phase. In this way, biosensors with relatively good electrochemical response have been built by a one-step electrodeposition method that grows the active phase from a chitosan–CNT–GOD solution [206]. In this approach the biopolymer acts as a continuous phase

in which CNTs and the enzyme are entrapped. In other approaches the enzyme and the CNTs are first precipitated onto the surface of the electrode, and then a polymer is deposited to wrap the active phase, thus avoiding its dispersion in the solution. One example of this method is the preparation of hybrid films of MWCNTs and hemoglobin incorporating poly(sodium-*p*-styrene-sulfonate) and cetyltrimethylammonium bromide [207]. Mioglobin has also been entrapped together with MWCNTs on a glassy carbon electrode with Nafion acting as agglutinant [208]. In both cases, the presence of CNTs in the film promotes electron transfer properties between the entrapped protein and the electrode, which could be of interest for the development of biosensors, catalytic bioreactors and other biomedical devices.

Although the electrical properties of CNTs are altered by modification of their surface, in certain cases the direct anchorage of the enzyme to the nanotubes has also been explored. These synthetic routes imply a previous activation of CNTs with acid to create carboxyl and hydroxy groups on their surface to which the positively charged species can be directly attached. Thus, poly(acrylonitrile-*co*-acrylic acid) (PANCAA) has been coupled to modified MWCNTs with the aim being to prepare nanofibrous membranes in which it is possible to further immobilize enzymes [209]. For instance, catalase has been successfully bonded to the activated membrane, resulting in higher enzyme loading and activity, possibly due to the high specific surface area and good electrical conductivity afforded by the CNTs (Figure 1.16). Alternatively, enzymes can be grafted to a biopolymer, such as chitosan, previously combined with CNTs and

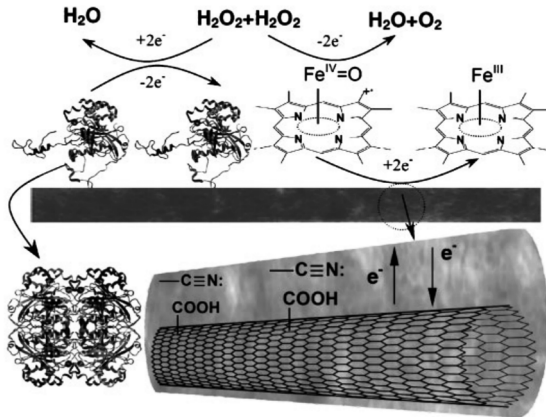
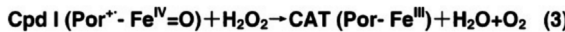
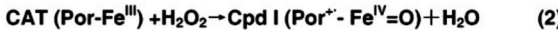


**Fig. 1.16** Schematic representation of the nanofibrous poly(acrylonitrile-*co*-acrylic acid) membrane containing MWCNTs, as well as the promoted electron transfer from hydrogen peroxide to the immobilized catalase through the PANCAA/MWCNTs nanofiber. Reprinted from [209] (reproduced by permission of Wiley-VCH).

processed as a film onto a glassy carbon electrode [210]. In this example, glucose dehydrogenase was bonded to chitosan using glutaric dialdehyde as a bridge between the amino groups of chitosan and the enzyme.

### 1.7

#### Bio-nanohybrids Based on Layered Transition Metal Solids

Vanadium pentoxide xerogel ( $\text{V}_2\text{O}_5 \cdot 1.6\text{H}_2\text{O}$ ) consists of  $\text{V}_2\text{O}_5$  layers arranged as stacked ribbon-like particles about 20 nm wide, 2 nm thick and 1  $\mu\text{m}$  long [211], containing water molecules and protons that allow the intercalation of a large variety of ions, molecules and polymers [212]. Several dipeptides such as Ala-Gln, Val-Gln and Ala-Gly (Figure 1.17A) can be intercalated in this host matrix by *in situ*

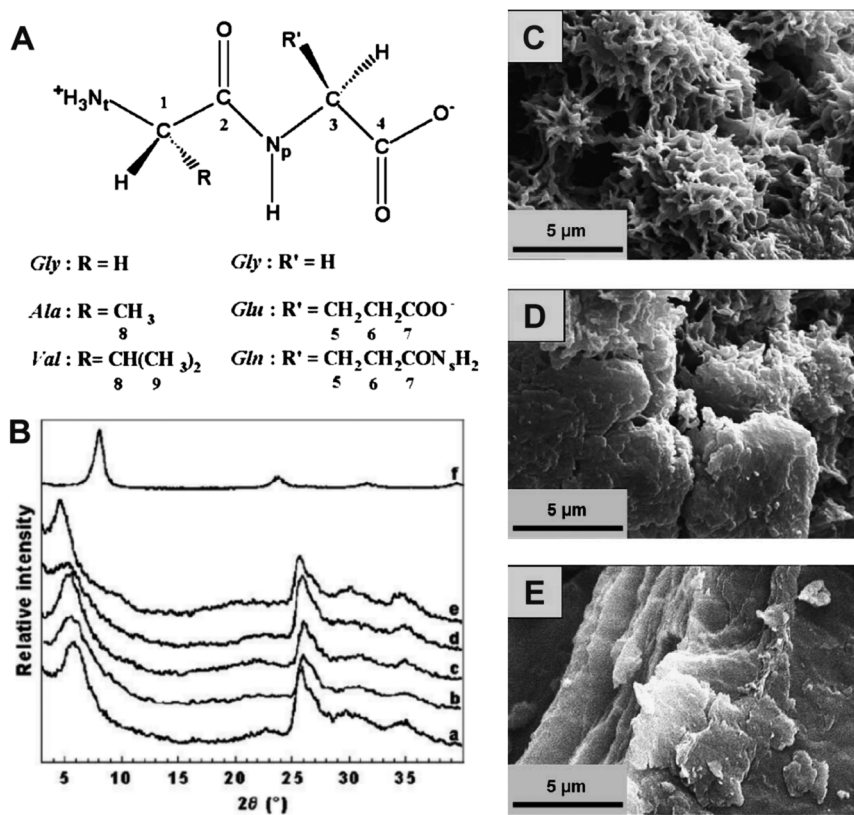


**Fig. 1.17** (A) Structure of the dipeptides Val-Gln, Ala-Gln, Ala-Gly, Gly-Gln and Gly-Glu. (B) X-ray diffraction patterns of the bio-nanohybrids including  $\text{V}_2\text{O}_5$  xerogel and (a) Ala-Gly, (b) Gly-Gln, (c) Ala-Gln, (d) Gly-Glu and (e) Val-Gln. (f) X-ray diffraction pattern of a  $\text{V}_2\text{O}_5 \cdot 1.8\text{H}_2\text{O}$  xer-

ogel film. SEM micrographs of the  $(\text{Ala-Gly})_{0.27}\text{V}_2\text{O}_5 \cdot 1.0\text{H}_2\text{O}$  hybrid synthesized at (C) pH = 1.5, and (D) pH = 1.0. (E) SEM micrograph of  $\text{V}_2\text{O}_5 \cdot 1.8\text{H}_2\text{O}$  xerogel. Adapted from [213] with permission from Elsevier.

synthesis of the hydrated vanadium pentoxide, as confirmed by X-ray diffraction (Figure 1.17B), that is by mixing the dipeptides with an acidified solution of sodium metavanadate. The resulting materials present a sponge-like morphology, as shown in Figure 1.17C, D, in which the peptide bonds between the amino acids are preserved despite the low pH of the system [213]. Melanin is a biomacromolecule mainly derived from cystine and tyrosine amino acids, usually associated with proteins in aggregates denoted as melanosomes. Two recent studies report the intercalation of a melanin-like compound (3,4-dihydroxy-phenylalanine) between the layers of vanadium pentoxide [214,215]. Both studies open the way to the preparation of melanin-based nanocomposites, which could profit from the interesting optical (UVabsorption) and solid-state electrical (photo- and semi-conductivity) properties of this biopolymer [123]. Other biomolecules with different functionality have been assembled with vanadium pentoxide xerogel, the aim being to develop new bio-nanocomposites with synergic properties afforded by both types of components. Chitosan intercalates  $V_2O_5$  xerogel leading to an increase in the interlayer distance of about 0.4 nm, which indicates the arrangement of the polysaccharide in a monolayer [216]. The potential interest of the resulting bio-nanocomposites is their use as the active phase in electrochemical sensors, in analogy to chitosan–clay nanocomposites [129,130]. The electrical conductivity provided by the inorganic counterpart can be expected to facilitate the electrochemical response. However, the oxidant character of  $V_2O_5$  xerogel may lead to biopolymer degradation to the detriment of the bio-nanocomposite stability and activity. It has been found that adsorption taking place only on the external surface of the layered solid results in microcomposite assemblies, increasing the stability of the systems in comparison to bio-nanocomposites formed by intercalation. This is the case for hybrid materials based on the immobilization of glucose oxidase on vanadium pentoxide [217].

Layered tetralkylammonium-modified manganese oxide shows the ability to intercalate myoglobin and hemoglobin that can retain their peroxidase activity [218]. Intercalation of methylcellulose into lithiated phases of manganese oxides was carried out through a mechanism of delamination–restacking giving rise to methyl cellulose– $Li_xMoO_3$  nanocomposites [219]. The presence of the insulating biopolymer between the inorganic layers decreases the inner conductivity of the pristine solid from  $10^{-2}$  to  $10^{-6}$  S/cm, preventing their potential use as electrodes for electrochemical devices. Further research to modulate the electrical conductivity of these bio-nanocomposites is required in order to develop new cathode materials for rechargeable Li-batteries.

Mixed oxides with a layered structure, such as calcium niobate perovskites exchanged with quaternary ammonium ions, can produce stable colloidal dispersion of the perovskite layers able to be assembled with biopolymers in aqueous solutions. For instance, assembly with gelatin leads to restacking of the perovskite nanosheets, which are homogeneously distributed in the biopolymer and highly oriented with the (*a*, *b*) plane parallel to the resulting films (Figure 1.18) [220]. These biohybrid films show an increase in dielectric permittivity that can be useful for application in the microwave industry or in high frequency devices. Similarly, hemoglobin has been intercalated as a mono- or bi-layer in tetrabutylammonium-modified layered niobate

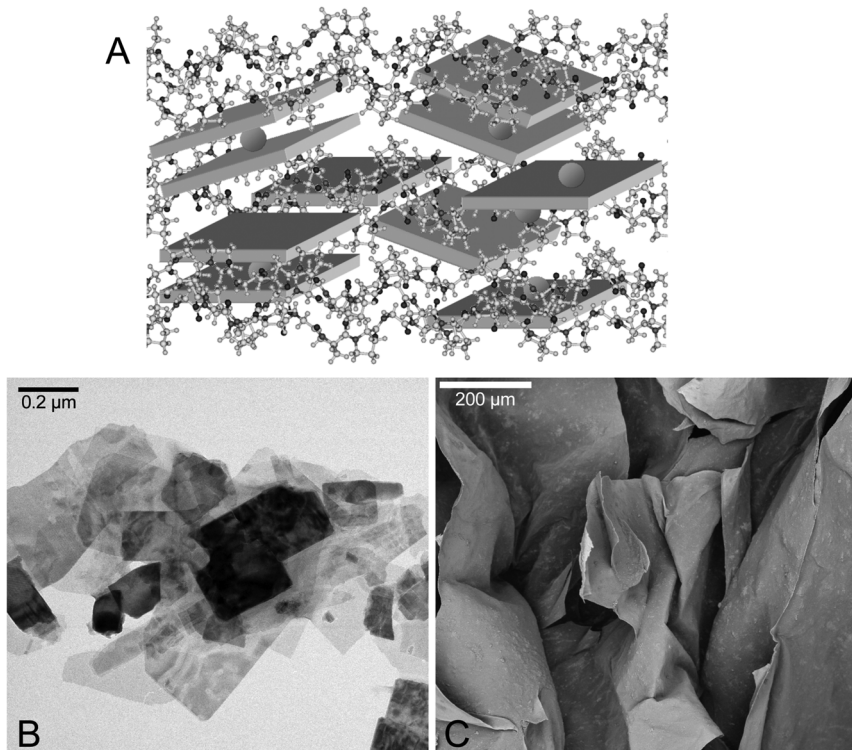


**Fig. 1.18** (A) Schematic representation of gelatin-perovskite bio-nanocomposite. (B) TEM image of TBA-modified perovskite and (C) SEM image of this TBA-perovskite after assembly with gelatin.

through a mechanism of delamination–restacking. The immobilization of this protein improves its thermal stability and enhances its activity in organic media [221].

Besides smectites, LDHs or vanadium pentoxide xerogel mentioned above, there are other layered inorganic hosts able to assemble biomolecules to give bio-nanocomposite materials. In this way certain transition metal phosphates and chalcogenides have been used to prepare hybrids involving structural and functional proteins [123]. For instance, gelatin can be intercalated into layered  $\alpha$ -zirconium phosphate ( $\text{Zr}(\text{HPO}_4)_2 \cdot n\text{H}_2\text{O}$ ) by treatment at acidic pH [222]. The process gives rise to a bio-nanocomposite that exhibits a basal spacing of 2.7 nm, due to the separation of the  $\alpha$ -zirconium phosphate layers by the protein chains. The same phosphate was used to intercalate lysozyme and protamine, which represent a class of globular proteins of medium and low molecular weight, respectively [222]. Similarly, Zr-phosphate nanocomposites including hemoglobin, myoglobin, lysozyme, chymotrypsin and glucose oxidase have been synthesized at pH 7.2, giving well defined intercalated compounds (Figure 1.19) [223]. The basal spacing values deduced from the XRD patterns are compatible with the molecular dimensions of the different intercalated proteins.

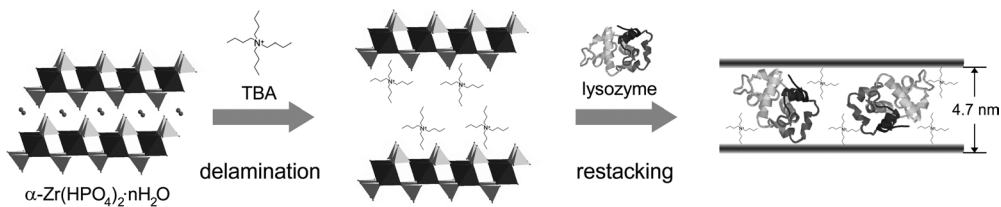


**Fig. 1.19** Intercalation of enzymes at the galleries of layered  $\alpha$ -zirconium phosphate following a delamination-restacking mechanism.

Transition-metal phosphorus trichalcogenides such as  $\text{MnPS}_3$  are able to intercalate amino acids and peptides by ion exchange. In this way, increases in the basal spacing of 0.7 and 3–4 nm are observed for the intercalation of poly-L-lysine and lysozyme, respectively [224]. Interestingly, the enzymatic activity of the immobilized protein has been detected, suggesting that the enzyme is protected against denaturation.

## 1.8

### Trends and Perspectives

Bio-nanohybrids represent an emerging group of advanced nanostructured materials that are receiving increasing interest in view of their versatility towards potential applications. The synthetic approaches that can be employed in the preparation of bio-nanocomposites may be principally based on detailed knowledge of the interfacial interactions between both components, that is biopolymers and inorganic solids. The mechanisms governing the assembly between the components, which can be the determining factor in the structural arrangement of the resulting materials, require further research. Within this context, understanding the biominerization processes that take place in nature can also assist in the development of new bio-nanohybrid materials. In this way, bio-nanocomposites, and their resulting properties, can ideally be tunable towards suitable characteristics that are necessary for specific applications.

Above we have shown the attractiveness of the so-called green nanocomposites, although the research on these materials can still be considered to be in an embryonic phase. It can be expected that diverse nano- or micro-particles of silica, silicates, LDHs and carbonates could be used as ecological and low cost “nanofillers” that can be assembled with polysaccharides and other biopolymers. The controlled modification of natural polymers can alter the nature of the interactions between components, affording new formulations that could lead to bioplastics with improved mechanical and barrier properties.

Another important group of bio-nanohybrids are the new materials needed for biomedical purposes, such as the development of artificial biological tissues and particularly those related to bone implants. Future progress within this field will require investigation of the use of nanoparticulate inorganic solids based on diverse ceramics, and even metal–ceramic composites, as an alternative to HAP and the related compounds currently employed. In this context, the use of multicomponent

polymeric and inorganic nanoparticulated systems could also be envisaged, employing techniques based on cryogenic synthesis to form assemblies with macroporosity useful for new materials for bone reparation. The use of bio-nanocomposites in DDS, including DNA non-viral vectors in gene therapy, also represents interesting biomedical applications of biohybrids. Alternative charged biopolymers coupled to diverse nanofillers (silica, phosphates, silicates, carbonates, etc.) appear attractive for the development of new biocompatible materials with the ability to uptake, carry and deliver molecular drugs in living organisms. By introducing magnetic properties, these bio-nanocomposites can be useful for drug transport to specific sites in the organs through guidance with external magnetic fields.

Among the new potential applications of bio-nanocomposites, we have highlighted that diverse inorganic components such as clay-based materials, metal nanoparticles and conductive carbon nanotubes can act as active phases in different type of devices, such as electrochemical sensors and biosensors. As certain inorganic solids have been employed as a protective matrix for the entrapment of living cells and enzymes, we can contemplate the extension of their use for the preparation of different bioactive nanocomposites that can be integrated in biosensors and bioreactors with a view to developing a new generation of advanced devices.

Finally, it can be envisaged that the future development of novel bio-nanohybrids will lead to new improved properties and multifunctionality derived from the synergistic combination of nanosized inorganic solids, with different structural and textural features, with molecular or even highly organized species of biological origin that are extraordinarily abundant in Nature.

### Acknowledgements

The authors acknowledge financial support from the CICYT, Spain (Project MAT2006-03356), and the Comunidad de Madrid, Spain (Project S-0505/MAT/000227).

### References

- 1 Dujardin, E. and Mann, S. (2002) *Advanced Materials*, **14**, 775–788.
- 2 Ruiz-Hitzky, E. and Darder, M. (eds) (2006) Special Issue on Trends in Biohybrid Nanostructured Materials, *Current Nanoscience*, **2**, 153–294.
- 3 Ruiz-Hitzky, E., Darder, M. and Aranda, P. (2005) *Journal of Materials Chemistry*, **15**, 3650–3662.
- 4 Darder, M., Aranda, P. and Ruiz-Hitzky, E. (2007) *Advanced Materials*, **19**, 1309–1319.
- 5 Darder, M., Aranda, P. and Ruiz-Hitzky, E. (2007) *Analés de Química*, **103**, 21–29.
- 6 Ray, S.S. and Bousmina, M. (2005) *Progress in Materials Science*, **50**, 962–1079.
- 7 Pandey, J.K., Kumar, A.P., Misra, M., Mohanty, A.K., Drzal, L.T. and Singh, R.P. (2005) *Journal of Nanoscience and Nanotechnology*, **5**, 497–526.

8 Fratzl, P., Gupta, H.S., Paschalis, E.P. and Roschger, P. (2004) *Journal of Materials Chemistry*, **14**, 2115–2123.

9 Su, X.W. and Cui, F.Z. (1999) *Materials Science and Engineering C*, **7**, 19–29.

10 Schaffer, T.E., Ionescu-Zanetti, C., Proksch, R., Fritz, M., Walters, D.A., Almqvist, N., Zaremba, C.M., Belcher, A.M., Smith, B.L., Stucky, G.D., Morse, D.E. and Hansma, P.K. (1997) *Chemistry of Materials*, **9**, 1731–1740.

11 Zaremba, C.M., Morse, D.E., Mann, S., Hansma, P.K. and Stucky, G.D. (1998) *Chemistry of Materials*, **10**, 3813–3824.

12 Smith, B.L., Schaffer, T.E., Viani, N., Thompson, J.B., Frederick, N.A., Kindt, J., Belcher, A., Stucky, G.D., Morse, D.E. and Hansma, P.K. (1999) *Nature*, **399**, 761–763.

13 Katti, D.R., Pradhan, S.M. and Katti, K.S. (2004) *Reviews on Advanced Materials Science*, **6**, 162–168.

14 Sellinger, A., Weiss, P.M., Nguyen, A., Lu, Y., Assink, R.A., Gong, W. and Brinker, C.J. (1998) *Nature*, **394**, 256–260.

15 Almqvist, N., Thomson, N.H., Smith, B.L., Stucky, G.D., Morse, D.E. and Hansma, P.K. (1999) *Materials Science and Engineering C*, **7**, 37–43.

16 Pezzotti, G., Asmus, S.M.F., Ferroni, L.P. and Miki, S. (2002) *Journal of Materials Science Materials in Medicine*, **13**, 783–787.

17 Tang, Z., Kotov, N.A., Magonov, S. and Ozturk, B. (2003) *Nature Materials*, **2**, 413–418.

18 Ruiz-Hitzky, E. (2003) *The Chemical Record*, **3**, 88–100.

19 Sanchez, C. (2001) Biomimetisme et Matériaux. Observatoire Française des Techniques Avancées, Série ARAGO 25, OFTA, Paris.

20 Wetherbee, R. (2002) *Science*, **298**, 547–547.

21 Sumper, M. and Brunner, E. (2006) *Advanced Functional Materials*, **16**, 17–26.

22 Coradin, T. and Livage, J. (2001) *Colloids and Surfaces B: Biointerfaces*, **21**, 329–336.

23 Coradin, T., Durupthy, O. and Livage, J. (2002) *Langmuir*, **18**, 2331–2336.

24 López, P.J., Gautier, C., Livage, J. and Coradin, T. (2005) *Current Nanoscience*, **1**, 73–83.

25 Ikoma, T., Muneta, T. and Tanaka, J. (2000) *Key Engineering Materials*, **192-1**, 487–490.

26 Kikuchi, M., Itoh, S., Ichinose, S., Shinomiya, K. and Tanaka, J. (2001) *Biomaterials*, **22**, 1705–1711.

27 Itoh, S., Kikuchi, M., Koyama, Y., Takakuda, K., Shinomiya, K. and Tanaka, J. (2004) *Cell Transplantation*, **13**, 451–461.

28 Berry, C. (2005) *Journal of Materials Chemistry*, **15**, 543–547.

29 Tartaj, P., Morales, M.P., Veintemillas-Verdaguer, S., González-Carreño, T. and Serna, C.J. (2003) *Journal of Physics D-Applied Physics*, **36**, R182–R197.

30 Retuert, J., Quijada, R., Arias, V. and Yazdani-Pedram, M. (2003) *Journal of Materials Research*, **18**, 487–494.

31 Darder, M., López-Blanco, M., Aranda, P., Aznar, A.J., Bravo, J. and Ruiz-Hitzky, E. (2006) *Chemistry of Materials*, **18**, 1602–1610.

32 Olmo, N., Lizarbe, M.A. and Gavilanes, J.G. (1987) *Biomaterials*, **8**, 67–69.

33 Olmo, N., Turnay, J., Herrera, J.I., Gavilanes, J.G. and Lizarbe, M.A. (1996) *Journal of Biomedical Materials Research*, **30**, 77–84.

34 Pérez-Castells, R., Alvarez, A., Gavilanes, J., Lizarbe, M.A., Martínez del Pozo, A., Olmo, N. and Santarén, J. (1987) (eds L.G. Schultz H. van Olphen, F.A. Mumpton), *Proceedings of the International Clay Conference*, Denver, 1985, The Clay Mineral Society, Bloomington, 359–362.

35 Narain, R., Housni, A. and Lane, L. (2006) *Journal of Polymer Science Part A: Polymer Chemistry*, **44**, 6558–6568.

**36** Poulsen, N., Sumper, M. and Kröger, N. (2003) *Proceedings of the National Academy of Sciences of the United States of America*, **100**, 12075–12080.

**37** Schröder, H.C., Boreiko, A., Korzhev, M., Tahir, M.N., Tremel, W., Eckert, C., Ushijima, H., Müller, I.M. and Müller, W.E.G. (2006) *Journal of Biological Chemistry*, **281**, (17), 12001–12009.

**38** Cha, J.N., Stucky, G.D., Morse, D.E. and Deming, T.J. (2000) *Nature*, **403**, 289–292.

**39** Patwardhan, S.V., Mukherjee, N., Steinitz-Kannan, M. and Clarson, S.J. (2003) *Chemical Communications*, 1122–1123.

**40** Belton, D., Paine, G., Patwardhan, S.V. and Perry, C.C. (2004) *Journal of Materials Chemistry*, **14**, 2231–2241.

**41** Sumper, M. and Kröger, N. (2004) *Journal of Materials Chemistry*, **14**, 2059–2065.

**42** Gautier, C., Lopez, P.J., Hemadi, M., Livage, J. and Coradin, T. (2006) *Langmuir*, **22**, 9092–9095.

**43** Coradin, T., Allouche, J., Boissière, M. and Livage, J. (2006) *Current Nanoscience*, **2**, 219–230.

**44** Coradin, T., Coupé, A. and Livage, J. (2003) *Colloids and Surfaces B Biointerfaces*, **29**, 189–196.

**45** Shchipunov, Y.A., Kojima, A. and Imae, T. (2005) *Journal of Colloid and Interface Science*, **285**, 574–580.

**46** Fuentes, S., Retuert, P.J., Gonzalez, G. and Ruiz-Hitzky, E. (1997) *International Journal of Polymeric Materials*, **35**, 61–70.

**47** Silva, S.S., Ferreira, R.A.S., Fu, L.S., Carlos, L.D., Mano, J.F., Reis, R.L. and Rocha, J. (2005) *Journal of Materials Chemistry*, **15**, 3952–3961.

**48** Rashidova, S.Sh., Shakarova, D.Sh., Ruzimuradov, O.N., Satubaldieva, D.T., Zalyalieva, S.V., Shpigun, O.A., Varlamov, V.P. and Kabulov, B.D. (2004) *Journal of Chromatography B*, **800**, 49–53.

**49** Livage, J., Coradin, T. and Roux, C. (2004) in *Functional Hybrid Materials* (P. Gómez-Romero and C. Sanchez) Wiley-VCH, Weinheim, Ch. 11.

**50** Boissière, M., Meadows, P.J., Brayner, R., Hélary, C., Livage, J. and Coradin, T. (2006) *Journal of Materials Chemistry*, **16**, 1178–1182.

**51** Boissière, M., Tourrette, A., Devoisselle, J.M., Di Renzo, F. and Quignard, F. (2006) *Journal of Colloid and Interface Science*, **294**, 109–116.

**52** Böttcher, H., Jagota, C., Trepte, J., Kallies, K.-H. and Haufe, H. (1999) *Journal of Controlled Release*, **60**, 57–65.

**53** Zhang, L. and Dong, S. (2006) *Analytical Chemistry*, **78**, 5119–5123.

**54** Jin, W. and Brennan, D. (2002) *Analytica Chimica Acta*, **461**, 1–36.

**55** Avnir, D., Coradin, T., Lev, O. and Livage, J. (2006) *Journal of Materials Chemistry*, **16**, 1013–1030.

**56** Frenkel-Mullerad, H. and Avnir, D. (2005) *Journal of the American Chemical Society*, **127**, 8077–8081.

**57** Gill, I. and Ballesteros, A. (2000) *Trends in Biotechnology*, **18**, 282–296.

**58** Ferrer, M.L., del Monte, F. and Levy, D. (2002) *Chemistry of Materials*, **14**, 3619–3621.

**59** Gill, I. and Ballesteros, A. (1998) *Journal of the American Chemical Society*, **120**, 8587–8598.

**60** Shchipunov, Y.A., Karpenko, T.Y., Bakunina, I.Y., Burtseva, Y.V. and Zvyagintseva, T.N. (2004) *Journal of Biochemical and Biophysical Methods*, **58**, 25–38.

**61** Darder, M., Colilla, M., Lara, N. and Ruiz-Hitzky, E. (2002) *Journal of Materials Chemistry*, **12**, 3660–3664.

**62** Fennouh, S., Guyon, S., Livage, J. and Roux, C. (2000) *Journal of Sol-Gel Science and Technology*, **19**, 647–649.

**63** Nassif, N., Roux, C., Coradin, T., Rager, M.N., Bouvet, O.M.M. and Livage, J. (2003) *Journal of Materials Chemistry*, **13**, 203–208.

**64** Nassif, N., Roux, C., Coradin, T., Bouvet, O.M.M. and Livage, J. (2004) *Journal of Materials Chemistry*, **14**, 2264–2268.

**65** Ferrer, M.L., Garcia-Carvajal, Z.Y., Yuste, L., Rojo, F. and del Monte, F. (2006) *Chemistry of Materials*, **18**, 1458–1463.

**66** Katagiri, K., Ariga, K. and Kikuchi, J.-I. (1999) *Chemistry Letters*, 661–662.

**67** Katagiri, K., Hamasaki, R., Ariga, K. and Kikuchi, J.-I. (2002) *Journal of the American Chemical Society*, **124**, 7892–7893.

**68** Katagiri, K., Hamasaki, R., Ariga, K. and Kikuchi, J.-I. (2003) *Journal of Sol-Gel Science and Technology*, **26**, 393–396.

**69** Ariga, K. (2004) *The Chemical Record*, **3**, 297–307.

**70** Ariga, K., Vinu, A. and Miyahara, M. (2006) *Current Nanoscience*, **2**, 197–210.

**71** Ruiz-Hitzky, E., Letaief, S. and Prévot, V. (2002) *Advanced Materials*, **14**, 439–443.

**72** <http://en.wikipedia.org/wiki/Ceramic>.

**73** Burgos-Asperilla, L., Darder, M., Aranda, P., Vázquez, L., Vázquez, M. and Ruiz-Hitzky, E. (2007) *Journal of Materials Chemistry*, DOI: 10.1039/b706011d.

**74** Murugan, R. and Ramakrishna, S. (2005) *Composites Science and Technology*, **65**, 2385–2406.

**75** Xu, A.-W., Ma, Y. and Cölfen, H. (2007) *Journal of Materials Chemistry*, **17**, 415–449.

**76** Ameye, L., DeBecker, G., Killian, C., Wilt, F., Kemps, R., Kuypers, S. and Dubois, P. (2001) *Journal of Structural Biology*, **134**, 56–66.

**77** Borelli, G., Mayer-Gostan, N., Merle, P. L., DePontual, H., Boeuf, G., Allemand, D. and Payan, P. (2003) *Calcified Tissue International*, **72**, 717–725.

**78** Raabe, D., Romano, P., Sachs, C., Al-Sawalmih, A., Brokmeier, H.-G., Yi, S.-B., Servos, G. and Hartwig, H.G. (2005) *Journal of Crystal Growth*, **283**, 1–7.

**79** Falini, G. (2000) *International Journal of Inorganic Materials*, **2**, 455–461.

**80** Kato, T., Sugawara, A. and Hosoda, N. (2002) *Advanced Materials*, **14**, 869–877.

**81** Manoli, F., Koutsopoulos, S. and Dalas, E. (1997) *Journal of Crystal Growth*, **182**, 116–124.

**82** Manoli, F. and Dalas, E. (1999) *Journal of Crystal Growth*, **204**, 369–375.

**83** Wang, W., Wang, G., Liu, Y., Zheng, C. and Zhan, Y. (2001) *Journal of Materials Chemistry*, **11**, 1752–1754.

**84** Gower, L.A. and Tirrell, D.A. (1998) *Journal of Crystal Growth*, **191**, 153–160.

**85** Neira-Carrillo, A., Yazdani-Pedram, M., Retuert, J., Diaz-Dosque, M., Gallois, S. and Arias, J.L. (2005) *Journal of Colloid and Interface Science*, **286**, 134–141.

**86** Kuang, M., Wang, D., Gao, M., Hartmann, J. and Möhwald, H. (2005) *Chemistry of Materials*, **17**, 656–660.

**87** Kato, T. (2000) *Advanced Materials*, **12**, 1543–1546.

**88** Sugawara, A. and Kato, T. (2000) *Chemical Communications*, 487–488.

**89** Wakayama, H., Hall, S.R. and Mann, S. (2005) *Journal of Materials Chemistry*, **15**, 1134–1136.

**90** Dorozhkin, S.V. and Epple, M. (2002) *Angewandte Chemie-International Edition*, **41**, 3130–3146.

**91** Palin, E., Liu, H. and Webster, T.J. (2005) *Nanotechnology*, **16**, 1828–1835.

**92** Thomas, V., Dean, D.R. and Vohra, Y.K. (2006) *Current Nanoscience*, **2**, 155–177.

**93** Widmer, M.S. and Mikos, A.G. (1998) in *Frontiers in Tissue Engineering* (eds C.W. Jr Patrick, A.G. Mikos, L.V. McIntire), Elsevier Science Ltd, Oxford, Ch. II.5.

**94** Yokoyama, A., Gelinsky, M., Kawasaki, T., Kohgo, T., König, U., Pompe, W. and Watari, F. (2005) *Journal of Biomedical*

Materials Research Part B, **75B**, 464–472.

**95** Wang, Y.J., Yang, C.R., Chen, X.F. and Zhao, N.R. (2006) *Advanced Engineering Materials*, **8**, 97–100.

**96** Tampieri, A., Sandri, M., Landi, E., Celotti, G., Roveri, N., Mattioli-Belmonte, M., Virgili, L., Gabbanelli, F. and Biagini, G. (2005) *Acta Biomaterialia*, **1**, 343–351.

**97** Parhi, P., Ramanan, A. and Ray, A.R. (2006) *Journal of Applied Polymer Science*, **102**, 5162–5165.

**98** Rusu, V.M., Ng, C.-H., Wilke, M., Tiersch, B., Fratzl, P. and Peter, M.G. (2005) *Biomaterials*, **26**, 5414–5426.

**99** Kong, L., Gao, Y., Lu, G., Gong, Y., Zhao, N. and Zhang, X. (2006) *European Polymer Journal*, **42**, 3171–3179.

**100** Nayar, S., Sinha, M.K., Basu, D. and Sinha, A. (2006) *Journal of Materials Science, Materials in Medicine*, **17**, 1063–1068.

**101** Ritzoulis, C., Scoutaris, N., Demetriou, E., Papademetriou, K., Kokkou, S., Stavroulias, S. and Panayiotou, C. (2004) *Journal of Biomedical Materials Research*, **71A**, 675–684.

**102** Ishikawa, Y., Komotori, J. and Senna, M. (2006) *Current Nanoscience*, **2**, 191–196.

**103** Senna, M. (2005) *Materials Science and Engineering A*, **412**, 37–42.

**104** Kino, R., Ikoma, T., Monkawa, A., Yunoki, S., Munekata, M., Tanaka, J. and Asakura, T. (2006) *Applied Polymer Science*, **99**, 2822–2830.

**105** Takeuchi, A., Ohtsuki, C., Miyazaki, T., Kamitakahara, M., Ogata, S.-I., Yamazaki, M., Furutani, Y., Kinoshita, H. and Tanihara, M. (2005) *Journal of the Royal Society Interface*, **2**, 373–378.

**106** Kothapalli, C.R., Shaw, M.T. and Wei, M. (2005) *Acta Biomaterialia*, **1**, 653–662.

**107** Mathieu, L.M., Mueller, T.L., Bourban, P.-E., Pioletti, D.P., Müller, R. and Månson, J.-A.E. (2006) *Biomaterials*, **27**, 905–916.

**108** Rezwan, K., Chen, Q.Z., Blaker, J.J. and Boccaccini, A.R. (2006) *Biomaterials*, **27**, 3413–3431.

**109** Deville, S., Saiz, E., Nalla, R.K. and Tomsia, A.P. (2006) *Science*, **311**, 515–518.

**110** Sotome, S., Uemura, T., Kikuchi, M., Chen, J., Itoh, S., Tanaka, J., Tateishi, T. and Shinomiya, K. (2004) *Materials Science and Engineering C*, **24**, 341–347.

**111** Liu, T.-Y., Chen, S.-Y., Li, J.-H. and Liu, D.-M. (2006) *Journal of Controlled Release*, **112**, 88–95.

**112** Vallet-Regí, M. and González-Calbet, J.M. (2004) *Progress in Solid State Chemistry*, **32**, 1–31.

**113** Zou, C., Weng, W.J., Deng, X.L., Cheng, K., Liu, X.G., Du, P.Y., Shen, G. and Han, G.R. (2005) *Biomaterials*, **26**, 5276–5284.

**114** Liu, H., Li, H., Cheng, W.J., Yang, Y., Zhu, M.Y. and Zhou, C.R. (2006) *Acta Biomaterialia*, **2**, 557–565.

**115** Aunoble, S., Clement, D., Frayssinet, P., Harmand, M.F. and LeHuec, J.C. (2006) *Journal of Biomedical Materials Research Part A*, **78A**, 416–422.

**116** Takagi, S., Chow, L.C., Hirayama, S. and Eichmiller, F.C. (2003) *Dental Materials*, **19**, 797–804.

**117** Xu, H.H.K. and Simon, C.G. (2005) *Biomaterials*, **26**, 1337–1348.

**118** Simon, P., Schwarz, U. and Kniep, R. (2005) *Journal of Materials Chemistry*, **15**, 4992–4996.

**119** Tlatlik, H., Simon, P., Kawska, A., Zahn, D. and Kniep, R. (2006) *Angewandte Chemie-International Edition*, **45**, 1905–1910.

**120** Bergaya, F., Theng, B.K.G. and Lagaly, G. (eds) (2006) *Handbook of Clay Science*, Elsevier, Amsterdam.

**121** Ruiz-Hitzky, E., Aranda, P. and Serratosa, J.M. (2004) in *Handbook of Layered Materials* (eds S.M. Auerbach, K.A. Carrado,

P.K.Dutta), Marcel Dekker, New York, pp. 91–154.

122 Ruiz-Hitzky, E. and Van Meerbeeck, A. (2006) in *Handbook of Clay Science* (eds F. Bergaya B.K.G. Theng, G. Lagaly), Elsevier, Amsterdam, Ch. 10.3.

123 Ruiz-Hitzky, E., Aranda, P. and Darder, M. (2007) in *Bottom-Up Nanofabrication: Supramolecules, Self-Assemblies, and Organized Films* (eds. Ariga, K. and Nalwa, H.S.) American Scientific Publishers 9, Ch. 73.

124 Bradley, W.F. (1945) *Journal of the American Chemical Society*, **67**, 975–981.

125 Greenland, D.J. (1956) *Journal of Soil Science*, **7**, 319–328.

126 Darder, M. and Ruiz-Hitzky, E. (2005) *Journal of Materials Chemistry*, **15**, 3913–3918.

127 Aranda, P., Darder, M., Fernández-Saavedra, R., López-Blanco, M. and Ruiz-Hitzky, E. (2006) *Thin Solid Films*, **495**, 104–112.

128 Bakandritsos, A., Steriotis, Th. and Petridis, D. (2004) *Chemistry of Materials*, **16**, 1551–1559.

129 Darder, M., Colilla, M. and Ruiz-Hitzky, E. (2003) *Chemistry of Materials*, **15**, 3774–3780.

130 Darder, M., Colilla, M. and Ruiz-Hitzky, E. (2005) *Applied Clay Science*, **28**, 199–208.

131 Xu, Y. and Hanna, M.A. Chitosan/clay nanocomposite films preparation and characterization Abstract in 2005 IFT Annual Meeting July 15–20, New Orleans, Louisiana.

132 Colilla, M. (2004) PhD Dissertation, Autonomous University of Madrid, Madrid.

133 Cohen, E., Joseph, T., Kahana, F. and Magdassi, S. (2003) *Photochemistry and Photobiology*, **77**, 180–185.

134 Chang, M.Y. and Juang, R.S. (2004) *Journal of Colloid and Interface Science*, **278**, 18–25.

135 Qiu, H.X., Yu, J.G. and Zhu, J.L. (2005) *Polymers and Polymer Composites*, **13**, 167–172.

136 Ogawa, M. and Kuroda, K. (1997) *Bulletin of the Chemical Society of Japan*, **70**, 2593–2618.

137 Ray, S.S. and Okamoto, M. (2003) *Macromolecular Rapid Communications*, **24**, 815–840.

138 Park, H.M., Misra, M., Drzal, L.T. and Mohanty, A.K. (2004) *Biomacromolecules*, **5**, 2281–2288.

139 Wibowo, A.C., Misra, M., Park, H.-M., Drzal, L.T., Schalek, R. and Mohanty, A. K. (2006) *Composites Part A: Applied Science and Manufacturing*, **37**, 1428–1433.

140 Kalambur, S. and Rizvi, S.S.H. (2005) *Journal of Applied Polymer Science*, **96**, 1072–1082.

141 Park, H.M., Mohanty, A.K., Drzal, L.T., Lee, E., Mielewski, D.F. and Misra, M. (2006) *Journal of Polymers and the Environment*, **14**, 27–35.

142 Maiti, P., Yamada, K., Okamoto, M., Ueda, K. and Okamoto, K. (2002) *Chemistry of Materials*, **14**, 4654–4661.

143 Paul, M.-A., Alexandre, M., Degeé, P., Henrist, C., Rulmont, A. and Dubois, P. (2003) *Polymer*, **44**, 443–450.

144 Paul, M.-A., Delcourt, C., Alexandre, M., Degeé, P., Monteverde, F., Rulmont, A. and Dubois, P. (2005) *Macromolecular Chemistry and Physics*, **206**, 484–498.

145 Pluta, M., Galeski, A., Alexandre, A., Paul, M.-A. and Dubois, P. (2002) *Journal of Applied Polymer Science*, **86**, 1497–1506.

146 Ray, S.S., Yamada, K., Okamoto, M. and Ueda, K. (2003) *Macromolecular Materials and Engineering*, **288**, 203–208.

147 Paul, M.-A., Delcourt, C., Alexandre, M., Degeé, P., Monteverde, F. and Dubois, P. (2005) *Polymer Degradation and Stability*, **87**, 535–542.

**148** Brauner, K. and Preisinger, A. (1956) *Mineralogy and Petrology*, **6**, 120–140.

**149** Santarén, J., Sanz, J. and Ruiz-Hitzky, E. (1990) *Clays and Clay Minerals*, **38**, 63–68.

**150** Ahlrichs, J.L., Serna, C. and Serratosa, J.M. (1975) *Clays and Clay Minerals*, **23**, 119–124.

**151** Ruiz-Hitzky, E. (2001) *Journal of Materials Chemistry*, **11**, 86–91.

**152** Darder, M. and Ruiz-Hitzky, E. (2007) in Clay-Based Polymer Nanocomposite, Clay Minerals Society, Vol. 14 (eds. Carrado, K.A. and Bergaya, F.), The Clay Minerals Society, Chantilly (Virginia, EEUU), Ch. 8.

**153** Gómez-Avilés, A., Darder, M., Aranda, P. and Ruiz-Hitzky, E. (2007) *Angewandte Chemie-International Edition*, **46**, 923–925.

**154** Chang, S.H., Ryan, M.E. and Gupta, R. K. (1991) *Journal of Applied Polymer Science*, **43**, 1293–1299.

**155** Li, A., Liu, R. and Wang, A. (2005) *Journal of Applied Polymer Science*, **98**, 1351–1357.

**156** Leroux, F., Gachon, J. and Besse, J.-P. (2004) *Journal of Solid State Chemistry*, **177**, 245–250.

**157** Darder, M., López-Blanco, M., Aranda, P., Leroux, F. and Ruiz-Hitzky, E. (2005) *Chemistry of Materials*, **17**, 1969–1977.

**158** Choy, J.H., Kwak, S.Y., Park, J.S., Jeong, Y.J. and Portier, J. (1999) *Journal of the American Chemical Society*, **121**, 1399–1400.

**159** Choy, J.H., Kwak, S.Y., Jeong, Y.J. and Park, J.S. (2000) *Angewandte Chemie-International Edition*, **39**, 4042–4045.

**160** Kwak, S.Y., Jeong, Y.J., Park, J.S. and Choy, J.H. (2002) *Solid State Ionics*, **151**, 229–234.

**161** Forano, C., Vial, S. and Mousty, C. (2006) *Current Nanoscience*, **2**, 283–294.

**162** Gleitsmann, T., Bernhardt, T.M. and Wöste, L. (2006) *Applied Physics A*, **82**, 125–130.

**163** Lee, S. and Pérez-Luna, V.H. (2005) *Analytical Chemistry*, **77**, 7204–7211.

**164** dosSantos, D.S., Jr, Goulet, P.J.G., Pieczonka, N.P.W., Oliveira, O.N. Jr, and Aroca, R.F. (2004) *Langmuir*, **20**, 10273–10277.

**165** Li, Z., Du, Y., Zhang, Z. and Pang, D. (2003) *Reactive and Functional Polymers*, **55**, 35–43.

**166** Brayner, R., Coradin, T., Fiévet-Vincent, F., Livage, J. and Fiévet, F. (2005) *New Journal of Chemistry*, **29**, 681–685.

**167** Srivastava, S., Samanta, B., Arumugam, P., Han, G. and Rotello, V. M. (2007) *Journal of Materials Chemistry*, **17**, 52–55.

**168** Cao, Y., Zhou, Y., Shan, Y., Ju, H. and Xue, X. (2006) *Advanced Materials*, **18**, 1838–1841.

**169** Katz, E., Shipway, A.N. and Willner, I. (2004) in Nanoparticles. From Theory to Applications (ed. G. Schmid), Wiley VCH, Weinheim, Ch. 6.

**170** Rawat, M., Singh, D. and Saraf, S. (2006) *Biological and Pharmaceutical Bulletin*, **29**, 1790–1798.

**171** Ha?eli, U., Schütt, W. and Teller, J., Zborowski, M. (eds) (1997) Scientific and Clinical Applications of Magnetic Carriers, Plenum Press, New York.

**172** Bergemann, C., Mullerschulte, D., Oster, J., Abrassard, L. and Lubbe, A.S. (1999) *Journal of Magnetism and Magnetic Materials*, **194**, 45–52.

**173** Gómez Lopera, S.A., Plaza, R.C. and Delgado, A.V. (2001) *Journal of Colloid and Interface Science*, **240**, 40–47.

**174** Arias, J.L., Gallardo, V., Gómez Lopera, S.A., Plaza, R.C. and Delgado, A.V. (2001) *Journal of Controlled Release*, **77**, 309–321.

**175** Tan, S.T., Wendorff, J.H., Pietzonka, C., Jia, Z.H. and Wang, G.Q. (2005) *ChemPhysChem*, **6**, 1461–1465.

176 Menager, C. and Cabuil, V. (1995) *Journal of Colloid and Interface Science*, **69**, 251–253.

177 Kuznetsov, A.A., Filippov, V.I., Alyautdin, R.N., Torshina, N.L. and Kuznetsov, O.A. (2001) *Journal of Magnetism and Magnetic Materials*, **225**, 95–100.

178 Luckarift, H.R., Dickerson, M.B., Sandhage, K.H. and Spain, J.C. (2006) *Small*, **2**, 640–643.

179 Lu, Y., Liu, Y., Xu, J., Xu, C., Liu, B. and Kong, J. (2005) *Sensors*, **5**, 258–265.

180 Hiroi, R., Ray, S.S., Okamoto, M. and Shiroi, T. (2004) *Macromolecular Rapid Communications*, **25**, 1359–1364.

181 Liu, T.-Y., Liao, H.-C., Lin, C.-C., Hu, S.-H. and Chen, S.-Y. (2006) *Langmuir*, **22**, 5804–5809.

182 Iijima, S. (1991) *Nature*, **354**, 56–58.

183 Shaito, R., Dresselhaus, G. and Dresselhaus, M.S. (1999) *Physical Properties of Carbon Nanotubes*, Imperial College Press, London.

184 Tjong, S.C. (2006) *Materials Science and Engineering: R: Reports*, **53**, 73–197.

185 Moniruzzaman, M. and Winey, K.I. (2006) *Macromolecules*, **39**, 5194–5205.

186 Coleman, J.N., Khan, U., Blau, W.J. and Gunko, Y.K. (2006) *Carbon*, **44**, 1624–1652.

187 Coleman, J.N., Khan, U. and Gunko, Y.K. (2006) *Advanced Materials*, **18**, 689–706.

188 Wang, S.-F., Shen, L., Zhang, W.-D. and Tong, Y.-L. (2005) *Biomacromolecules*, **6**, 3067–3072.

189 Shieh, Y.-T. and Yang, Y.-F. (2006) *European Polymer Journal*, **42**, 3162–3170.

190 Spinks, G.M., Shin, S.R., Wallace, G. G., Whitten, P.G., Kim, S.I. and Kim, S. J. (2006) *Sensors and Actuators B: Chemical*, **115**, 678–684.

191 Hasegawa, H., Fujisaka, T., Numata, M., Umeda, M., Matsumoto, T., Kimura, T., Okumura, S., Sakurai, K. and Shinkai, S. (2004) *Chemical Communications*, 2150–2151.

192 Chen, X., Lee, G.S., Zettl, A. and Bertozzi, C.R. (2004) *Angewandte Chemie-International Edition*, **43**, 6112–6116.

193 Matsura, K., Hayashi, K. and Kinmizuka, N. (2003) *Chemistry Letters*, **32**, 212–213.

194 Gu, L., Elkin, T., Jiang, X., Li, H., Qu, L., Tzeng, T.-Z.J., Joseph, R. and Sun, Y.-P. (2005) *Chemical Communications*, 874–876.

195 Dohi, H., Kikuchi, S., Kuwahara, S., Sugai, T. and Shinohara, H. (2006) *Chemical Physics Letters*, **428**, 98–101.

196 Kam, N.W., OConnell, M., Wisdom, J. A. and Dai, H. (2005) *Proceedings of the National Academy of Sciences of the United States of America*, **102**, 11600–11605.

197 Li, X., Peng, Y. and Qu, X. (2006) *Nucleic Acids Research*, **34**, 3670–3676.

198 Koyama, S., Haniu, H., Osaka, K., Koyama, H., Kuroiwa, N., Endo, M., Kim, Y.A. and Hayashi, T. (2006) *Small*, **2**, 1406–1411.

199 Smart, S.K., Cassady, A.I., Lu, G.Q. and Martin, D.J. (2006) *Carbon*, **44**, 1034–1047.

200 Tao, F., Gonzalez-Flecha, B. and Kobzik, L. (2003) *Free Radical Biology and Medicine*, **35**, 327–340.

201 Polizzi, S., Maugey, M., Poulin, S., Polulin, P. and Yahia, L.H. (2006) *Applied Surface Science*, **252**, 6750–6753.

202 Shi, X.F., Hudson, J.L., Spicer, P.P., Tour, J.M., Krishnamoorti, R. and Mikos, A.G. (2006) *Biomacromolecules*, **7**, 2237–2242.

203 Zhang, D., Kandadai, M.A., Cech, J.H., Roth, S. and Curran, S.A. (2006) *Journal of Physical Chemistry B*, **110**, 12910–12915.

204 Wang, Y.D., Joshi, P.P., Hobbs, K.L., Johnson, M.B. and Schmidtke, D.W. (2006) *Langmuir*, **22**, 9776–9783.

205 Liu, G.D. and Lin, Y.H. (2006) *Journal of Nanoscience and Nanotechnology*, **6**, 948–953.

**206** Luo, X.-L., Xu, J.-J., Wang, J.-L. and Chen, H.-Y. (2005) *Chemical Communications*, 2169–2171.

**207** Chen, L. and Lu, G. (2006) *Journal of Electroanalytical Chemistry*, **597**, 51–59.

**208** Li, Y., Lin, X. and Jiang, C. (2006) *Electroanalysis*, **18**, 2085–2091.

**209** Wang, Z.-G., Xu, Z.-K., Wan, L.-S., Wu, J., Innocent, C. and Seta, P. (2006) *Macromolecular Rapid Communications*, **27**, 516–521.

**210** Zhang, M., Smith, A. and Gorki, W. (2004) *Analytical Chemistry*, **76**, 5045–5050.

**211** Livage, J. (1991) *Chemistry of Materials*, **3**, 578–593.

**212** Rojas-Cervantes, M.L., Casal, B., Aranda, P., Savirón, M., Galván, J.C. and Ruiz-Hitzky, E. (2001) *Colloid and Polymer Science*, **279**, 990–1004.

**213** Durupthy, O., Steunou, N., Coradin, T. and Livage, J. (2006) *Journal of the Physics and Chemistry of Solids*, **67**, 944–949.

**214** Oliveira, H.P., Graeff, C.F.O., Zanta, C.L.P.S., Galina, A.C. and Gonçalves, P.J. (2000) *Journal of Materials Chemistry*, **10**, 371–375.

**215** Arashiro, E., Zampronio, E.C., Brunello, C.A., Lassali, T.A.F., Oliveira, H.P. and Graeff, C.F.O. (2001) *International Journal of Inorganic Materials*, **3**, 727–731.

**216** Darder, M., Aranda, P. and Ruiz-Hitzky, E., unpublished results.

**217** Gleezer, V. and Lev, O. (1993) *Journal of the American Chemical Society*, **115**, 2533–2534.

**218** Gao, Q., Suib, S.L. and Rusling, J.F. (2002) *Chemical Communications*, 2254–2255.

**219** Wang, L., Schindler, J., Kannefur, C.R. and Kanatzidis, M.G. (1997) *Journal of Materials Chemistry*, **7**, 1277–1283.

**220** Ruiz, A.I., Darder, M., Aranda, P., Jiménez, R., Van Damme, H. and Ruiz-Hitzky, E. (2006) *Journal of Nanoscience and Nanotechnology*, **6**, 1602–1610.

**221** Gao, L., Gao, Q., Wang, Q., Peng, S. and Shi, J. (2005) *Biomaterials*, **25**, 5267–5275.

**222** Ding, Y., Jones, D.J., Maireles-Torres, P. and Rozière, J. (1995) *Chemistry of Materials*, **7**, 562–571.

**223** Kumar, C.V. and Chaudari, A. (2000) *Journal of the American Chemical Society*, **122**, 830–837.

**224** Coradin, T., Coupé, A. and Livage, J. (2003) *Journal of Materials Chemistry*, **13**, 705–707.